



Titre: Far-from-cutoff conditions in cylindrical dielectric three-layer
Title: waveguide

Auteur: Jian Huang
Author:

Date: 2006

Type: Mémoire ou thèse / Dissertation or Thesis

Référence: Huang, J. (2006). Far-from-cutoff conditions in cylindrical dielectric three-layer
Citation: waveguide [Mémoire de maîtrise, École Polytechnique de Montréal]. PolyPublie.
<https://publications.polymtl.ca/7716/>

 **Document en libre accès dans PolyPublie**
Open Access document in PolyPublie

URL de PolyPublie: <https://publications.polymtl.ca/7716/>
PolyPublie URL:

**Directeurs de
recherche:**
Advisors:

Programme: Non spécifié
Program:

NOTE TO USERS

This reproduction is the best copy available.

UMI[®]

UNIVERSITÉ DE MONTRÉAL

FAR-FROM-CUTOFF CONDITIONS IN CYLINDRICAL
DIELECTRIC THREE-LAYER WAVEGUIDE

JIAN HUANG
DÉPARTMENT DE GÉNIE PHYSIQUE
ÉCOLE POLYTECHNIQUE DE MONTRÉAL

MÉMOIRE PRÉSENTÉ EN VUE DE L'OBTENTION
DU DIPLÔME DE MAÎTRISE ÈS SCIENCES APPLIQUÉES
(GÉNIE PHYSIQUE)
FÉVRIER 2006



Library and
Archives Canada

Bibliothèque et
Archives Canada

Published Heritage
Branch

Direction du
Patrimoine de l'édition

395 Wellington Street
Ottawa ON K1A 0N4
Canada

395, rue Wellington
Ottawa ON K1A 0N4
Canada

Your file Votre référence

ISBN: 978-0-494-17947-5

Our file Notre référence

ISBN: 978-0-494-17947-5

NOTICE:

The author has granted a non-exclusive license allowing Library and Archives Canada to reproduce, publish, archive, preserve, conserve, communicate to the public by telecommunication or on the Internet, loan, distribute and sell theses worldwide, for commercial or non-commercial purposes, in microform, paper, electronic and/or any other formats.

The author retains copyright ownership and moral rights in this thesis. Neither the thesis nor substantial extracts from it may be printed or otherwise reproduced without the author's permission.

AVIS:

L'auteur a accordé une licence non exclusive permettant à la Bibliothèque et Archives Canada de reproduire, publier, archiver, sauvegarder, conserver, transmettre au public par télécommunication ou par l'Internet, prêter, distribuer et vendre des thèses partout dans le monde, à des fins commerciales ou autres, sur support microforme, papier, électronique et/ou autres formats.

L'auteur conserve la propriété du droit d'auteur et des droits moraux qui protègent cette thèse. Ni la thèse ni des extraits substantiels de celle-ci ne doivent être imprimés ou autrement reproduits sans son autorisation.

In compliance with the Canadian Privacy Act some supporting forms may have been removed from this thesis.

Conformément à la loi canadienne sur la protection de la vie privée, quelques formulaires secondaires ont été enlevés de cette thèse.

While these forms may be included in the document page count, their removal does not represent any loss of content from the thesis.

Bien que ces formulaires aient inclus dans la pagination, il n'y aura aucun contenu manquant.


Canada

UNIVERSITÉ DE MONTRÉAL
ÉCOLE POLYTECHNIQUE DE MONTRÉAL

Ce mémoire intitulé:

FAR-FROM-CUTOFF CONDITIONS IN CYLINDRICAL
DIELECTRIC THREE-LAYER WAVEGUIDE

présenté par: HUANG Jian

en vue de l'obtention du diplôme de: Maîtrise ès sciences appliquées

a été dûment accepté par le jury d'examen constitué de:

M. MACIEJKO Romain, Ph.D., président

M. BURES Jacques, D.Sc, membre et directeur de recherche

M. GODBOUT Nicolas, Ph.D., membre

Acknowledgments

There are a lot of people I would like to thank for helping me to complete this thesis. First and foremost, I would like to thank Professor Jacques Bures for his tireless efforts and unending caring and generosity. I would also like to thank my wonderful wife for her support. I would like to dedicate this thesis to her.

Summary

Optical fiber plays a critical role as transmission media in the modern optical communication. Light traveling in the optical fiber is processed as an electromagnetic wave propagating in a cylindrical dielectric waveguide.

The propagating light in the dielectric waveguide is described as bound modes, which are the solution of Maxwell's equation subject to boundary conditions. The waveguide modes are classified into axial symmetric transverse mode, TE and TM modes, and hybrid HE and EH modes. Mode classification in cylindrical dielectric waveguides has always been important to the investigation of modes in optical fiber.

The ordinary optical fiber is typically a two layer structure where an infinite radius of cladding is assumed. The modal characteristics of the optical fiber have been studied extensively; however, if the radius of the outer cladding is not big enough, the two layer structure becomes a three layer structure.

Mode classification in three layer dielectric waveguides has been studied extensively in many previous articles. *A. Safaai-Jazi and al*⁸ and *Achint Kapoor and G. S. Singh*¹³, propose a generalized eigenvalue

equation which can be used to investigate the modal characteristics in the three layer structures. With the obtained eigenvalue equation, the cutoff condition of modes in three layer dielectric waveguides can be obtained at the limit where the modal parameter W tends to zero.

There is hardly any mention of the far-from-cutoff condition in the three layer dielectric waveguides. Guided by Professor *Jacques Bures's*¹⁷ proposal, this work tries to define a value range bounded by the cutoff and the far-from-cutoff conditions. The effective index of mode varies in this closed range. This limited range makes it easier to investigate the modal characteristics in a three layer structure more precisely.

As modal parameter tends to infinity, all the modal power is confined in the core. This is called far-from-cutoff condition of mode in waveguides.

The analytical far-from-cutoff expression is found with the previously obtained eigenvalue equation and through a lot of mathematical deductions at the limitation of $W \rightarrow \infty$.

Two methods are employed to prove the correctness of the far-from-cutoff expression. The first one is reduction method. The obtained far-from-cutoff condition in three layer structures is reduced by setting the radius of the first cladding to that of the core. The reduced far-from-cutoff expression in three layer structures is identical to the

far-from-cutoff expression in two layer structures. The second method is numerical calculation. The far-from-cutoff value is plotted with cutoff value and effective index together vs. the reduction factor (homothetic reduction factor of the transversal dimensions of the fiber). The figures show that the effective index varies in the range bounded by the cutoff and the far-from-cutoff conditions. It proves the validity of the proposal of Professor *Jacques Bures* and the correctness of the far-from-cutoff expression obtained in this paper.

The work of this paper is the first which gives the analytic far-from-cutoff expression of modes in three layers structure. It also makes it possible to investigate modal characteristics of three layers structure in a limited value range bounded by the cutoff and the far-from-cutoff conditions.

Abstract

This paper proposes that the far-from-cutoff condition can form a value range with the cutoff condition, in which the effective index falls. To investigate the modal characteristics of three layer dielectric waveguides, an analytic far-from-cutoff expression of three layer dielectric waveguides is presented. The far-from-cutoff expression is obtained with the method of eigenvalue equation. This paper is the first which derives the far-from-cutoff condition of three layer structures.

The obtained far-from-cutoff condition forms a value range with the cutoff condition to include the effective index. The effective index of mode varies in the value range bounded by the cutoff and the far-from-cutoff condition. It makes it easier to investigate the modal characteristics in a limited range more precisely.

This paper is a supplement of previous works of mode designation in three layer dielectric waveguides.

To prove the correctness of the analytic far-from-cutoff expression, two methods have been employed. One is to reduce the three layer structure into two layer structures by letting the radius of first cladding to tend to the radius of core. The far-from-cutoff expression obtained with

this method is identical to the far-from-cutoff expression obtained before in the two layer structures. The second method is the numerical calculation. The numerical calculation results are plotted with the cutoff condition and effective index together. The figures show that the effective index varies in the range bounded by the cutoff and the far-from-cutoff conditions. Both methods do well in proving that the obtained the far-from-cutoff expression is correct and can be used to form a value range to include the effective index.

Condensé en Français

1. Introduction

La fibre optique en verre ou en plastique est certainement le milieu idéal pour transmettre des communications par optique guidée. C'est principalement dû à la stabilité physique et chimique du milieu, à l'insensibilité aux interférences électromagnétiques, à la grande bande passante et aux très faibles pertes de signal observées principalement au voisinage de la longueur d'onde d'opération de $1.55\ \mu\text{m}$.

Le calcul, la nomenclature et la classification des modes vectoriels guidés dans les guides d'ondes diélectriques cylindriques sont très importants pour le développement des recherches sur les fibres optiques. Excepté pour les modes TE_{0m} et TM_{0m} transverses à symétrie axiale ayant respectivement des composantes longitudinales e_z et h_z nulles, tous les autres modes notés HE_{vm} et EH_{vm} sont hybrides et ont des composantes longitudinales non nulles.

Pour la fibre optique à saut d'indice à deux couches (cœur et gaine infinie), on peut montrer facilement que l'équation aux valeurs propres ou équation de dispersion peut se mettre sous une forme

quadratique avec un choix de signe pour les racines, ce qui permet de différencier les HE des EH . *Snyder et Lowe* ont étudié les limites de l'équation aux valeurs propres à la coupure puis loin de la coupure des modes, c'est-à-dire respectivement quand le paramètre de gaine $W \rightarrow 0$ et $W \rightarrow \infty$. Ainsi, on est en mesure de borner chaque solution modale ce qui permet de calculer directement n'importe quel mode sans être obligé de considérer et de numéroter toute la série des racines.

Lorsque la gaine est finie en présence d'un milieu extérieur, la fibre optique devient un guide d'onde diélectrique à trois couches et, selon les valeurs des indices, on peut obtenir des profils en escalier, en W ou en anneau. À chaque profil va maintenant correspondre des équations aux valeurs propres différentes, ce qui rend la classification et les calculs des modes beaucoup plus compliqués. Toutefois, on montre que l'on peut garder la même classification TE , TM , HE et EH et que ces équations peuvent encore se mettre sous une forme quadratique, ce qui permet de différencier les HE des EH , comme pour le cas des deux couches. *Safaai-Jazi et Yip*^{8 9} ont proposé une équation aux valeurs propres généralisée pour les profils à trois couches. Ils ont déterminé les limites de ces équations pour les quatre familles TE , TM , HE et EH à la coupure, lorsque le paramètre modal du milieu extérieur $W \rightarrow 0$. Ceci donne l'une des deux bornes de calcul, mais il manque l'autre qui n'a

pas été abordée par ces auteurs, c'est-à-dire le calcul des limites de ces équations loin de la coupure. Nous croyons qu'il est important de borner chaque solution du guide d'onde à trois couches avant d'effectuer le calcul final.

Le but de ce mémoire est de compléter le travail de *Safaai-Jazi et Yip*⁸⁻⁹ en trouvant les limites des équations aux valeurs propres loin de la coupure puis de borner et finalement de calculer les indices effectifs de différents modes. À titre d'exemple, on a pris la fibre SMF28™ opérant à $\lambda = 1.55\mu\text{m}$ avec un profil effilé caractérisé par différents facteurs de réduction R .

L'équation aux valeurs propres est obtenue en écrivant la continuité de deux composantes tangentielles et longitudinales à chacune des deux interfaces. Ceci conduit à une matrice 8×8 dont le déterminant doit être nul : c'est l'équation aux valeurs propres. Les conditions à la coupure sont obtenues quand le paramètre modal du milieu extérieur $W \rightarrow 0$, soit quand l'indice effectif \rightarrow l'indice extérieur. Par contre, les conditions loin de la coupure sont obtenues quand $W \rightarrow \infty$, soit pour le rayon de la gaine $\rightarrow \infty$, mais avec le paramètre modal de la gaine qui doit rester fini (de la même façon que le paramètre modal de cœur restait fini pour le profil à deux couches), ce qui implique que l'indice effectif

→ l'indice de gaine.

On détermine de cette façon les limites des équations aux valeurs propres pour les quatre familles de modes à la coupure et loin de la coupure. On en déduit ensuite les bornes de calcul pour chaque mode.

2. Équations aux valeurs propres

Comme tous les phénomènes électromagnétiques, la propagation de la lumière dans les fibres optiques est régit par les équations de Maxwell. Le facteur $\exp[i(\omega t - \beta z)]$ qui apparaît dans les expressions des champs électrique et magnétique et qui provient de l'invariance en translation du guide et de la dépendance temporelle, est omis par la suite. Pour une fibre idéale à sauts d'indice, les équations de Maxwell conduisent aux deux équations d'onde scalaires appliquées aux deux composantes longitudinales e_z et h_z

$$\begin{cases} \nabla_t^2 e_z + \{n^2 k^2 - \beta^2\} e_z = 0 \\ \nabla_t^2 h_z + \{n^2 k^2 - \beta^2\} h_z = 0 \end{cases} \quad (1)$$

où k est nombre d'onde dans le vide $k = 2\pi/\lambda_0$ et β la constante de propagation axiale ou valeur propre d'un mode du guide. En factorisant les solutions en r et Φ et en se servant de l'invariance en rotation, on

obtient pour chaque couche d'indice l'équation différentielle en r

$$\frac{d^2 R(r)}{dr^2} + \frac{1}{r} \frac{dR(r)}{dr} + \left[k_0^2 (n_j^2 - n_{eff}^2) - \frac{\nu^2}{r^2} \right] R(r) = 0 \quad (2)$$

où j représente le numéro de la couche d'indice n_j et $R(r)$ est le profil radial des champs e_z et h_z .

Pour les profils à sauts d'indice à trois couches, e_z et h_z s'expriment par des combinaisons de fonctions de Bessel ou de fonctions modifiées de Bessel de première et seconde espèces. Le choix de ces fonctions dépend du signe de $n_j^2 - n_{eff}^2$. Ainsi pour $n_j > n_{eff}$, (2) n'est autre que l'équation différentielle des fonctions de Bessel de première et seconde espèces dont les solutions sont des combinaisons linéaires de J_ν et Y_ν . Par contre, si $n_j < n_{eff}$, (2) est l'équation différentielle des fonctions modifiées de Bessel de première et seconde espèces dont les solutions sont des combinaisons de I_ν et K_ν .

Pour chaque couche, on exprime les composantes imaginaires e_z et h_z à l'aide de ces combinaisons linéaires avec des coefficients inconnus. Ensuite, on en déduit deux composantes transverses tangentielles réelles du champ électrique et magnétique qui s'expriment à l'aide des dérivées de e_z et h_z par rapport à r et Φ .

En écrivant les continuités de ces quatre composantes aux deux

interfaces, on en déduit huit équations linéaires reliant les huit coefficients inconnus. Le système se met sous la forme matricielle

$$\bar{A}\bar{I} = \bar{O} \quad (3)$$

où \bar{O} est la matrice zéro, \bar{A} une matrice 8x8 de coefficients connus et \bar{I} la matrice colonne des huit coefficients inconnus.

La solution non triviale de (3), c'est-à-dire autre que $\bar{I} = 0$, est donnée par le déterminant nul de \bar{A} . Ceci conduit à l'équation aux valeurs propres qui peut se mettre sous une forme quadratique dont les solutions générales sont

$$\bar{\eta}_1 = \frac{\nu}{\bar{x}^2} + \left\{ -G_2 \pm \left[(G_2')^2 + 4\varepsilon_1(\varepsilon_2 T)^2 \right]^{1/2} \right\} / 2G_1 \quad (4)$$

$$\begin{aligned} G_1 &= \varepsilon_1 \varepsilon_2 H_1 \\ G_2 &= H_2 && \text{avec le signe +} \\ G_2' &= H_2 && \text{avec le signe -} \end{aligned} \quad (5)$$

$$T = \nu n_{eff} \left[\left(\frac{1}{\bar{x}^2} - \frac{1}{\bar{U}_1^2} \right) H_1 + \varepsilon_2 \left(\frac{1}{\bar{U}_2^2} - \frac{1}{\bar{W}^2} \right) \bar{\Delta}_4 \right] \quad (6)$$

$$\begin{aligned} H_1 &= (\varepsilon_2 \bar{\Delta}_2 - \varepsilon_3 \bar{\Delta}_5) (\bar{\Delta}_2 - \bar{\Delta}_5) \\ &- \nu (\xi - 1) \left\{ \frac{[2\varepsilon_2 \bar{\Delta}_2 - (\varepsilon_2 + \varepsilon_3) \bar{\Delta}_5]}{\bar{U}_2^2} - \frac{[(\varepsilon_2 + \varepsilon_3) \bar{\Delta}_2 - 2\varepsilon_3 \bar{\Delta}_5]}{\bar{W}^2} \right\} \end{aligned} \quad (7)$$

$$\begin{aligned}
H_2 = \varepsilon_2 \left\{ \nu(\varepsilon_1 \pm \varepsilon_2) \frac{H_1}{\bar{U}_1^2} - \nu \varepsilon_2 \bar{\Delta}_4 \left[\frac{(\varepsilon_1 \pm \varepsilon_2)}{\bar{U}_2^2} - \frac{(\varepsilon_1 \pm \varepsilon_3)}{\bar{W}^2} \right] \right. \\
+ \nu(\varepsilon_1 \pm \varepsilon_2)(\xi - 1) \left[\bar{\Delta}_3 \left(\frac{2\varepsilon_2}{\bar{U}_2^2} - \frac{(\varepsilon_2 + \varepsilon_3)}{\bar{W}^2} \right) + \bar{\Delta}_1 \bar{\eta}_6 \left(\frac{(\varepsilon_2 + \varepsilon_3)}{\bar{U}_2^2} - \frac{2\varepsilon_3}{\bar{W}^2} \right) \right] \\
\left. - \varepsilon_1(\varepsilon_2 \bar{\Delta}_2 - \varepsilon_3 \bar{\Delta}_5)(\bar{\Delta}_3 + \bar{\Delta}_1 \bar{\eta}_6) \mp \varepsilon_2(\bar{\Delta}_2 - \bar{\Delta}_5)(\varepsilon_2 \bar{\Delta}_3 + \varepsilon_3 \bar{\Delta}_1 \bar{\eta}_6) \right\} \quad (8)
\end{aligned}$$

où les différents paramètres sont définis dans l'article de *Safaai-Jazi et Yip*.

Le choix de signe « + » ou « - » dans les expressions définit respectivement les deux familles de modes hybrides *EH* et *HE*. Le mode n'ayant pas de coupure et correspondant à la valeur d'indice effectif la plus grande est traditionnellement noté *HE*₁₁. Le groupe de solutions auquel il appartient constitue la famille des *HE*.

Les équations aux valeurs propres des modes *TE* et *TM* se déduisent des précédentes en faisant $\nu = 0$, ce qui donne

$$\varepsilon_1 \bar{\eta}_1 (\varepsilon_2 \bar{\Delta}_2 - \varepsilon_3 \bar{\Delta}_5) - \varepsilon_2^2 \bar{\Delta}_3 - \varepsilon_2 \varepsilon_3 \bar{\Delta}_1 \bar{\eta}_6 = 0 \quad \text{pour les modes } TM, \quad (9)$$

$$\bar{\eta}_1 (\bar{\Delta}_2 - \bar{\Delta}_5) - \bar{\Delta}_3 - \bar{\Delta}_1 \bar{\eta}_6 = 0 \quad \text{pour les modes } TE. \quad (10)$$

Ces équations ont des racines multiples. Les modes sont notés *TE*_{0*m*}, *TM*_{0*m*}, *HE* _{νm} et *EH* _{νm} . ν est le paramètre figurant dans l'équation (4) qui détermine l'ordre des fonctions de Bessel ou de Bessel modifiées alors que *m* est le numéro de la solution en commençant le numérotage par l'indice effectif le plus élevé.

3. Limites à la coupure

Proche de la coupure, la puissance modale a tendance à s'étaler dans le milieu extérieur. Au delà, le mode guidé est coupé et devient mode de radiation. Lorsque l'on est proche de la coupure, toutes les équations aux valeurs propres tendent vers des limites obtenues quand le paramètre modal du milieu extérieur $W \rightarrow 0$, soit $n_{\text{eff}} \rightarrow n_3$.

Ces équations limites sont successivement pour les *TE* et *TM*

$$\varepsilon_1 \bar{\eta}_1 (\xi - 1) + \varepsilon_2 \bar{\Delta}_1 = 0 \quad \text{pour les modes } TM, \quad (11)$$

$$\bar{\eta}_1 (\xi - 1) + \bar{\Delta}_1 = 0 \quad \text{pour les modes } TE. \quad (12)$$

Pour les modes hybrides *HE* et *EH*, il vient

$$\bar{\eta}_1 = \frac{\nu}{\bar{x}^2} + \left\{ E_2 \pm \sigma \left[\left(E_2' \right)^2 + 4\varepsilon_1 \varepsilon_3 E_3^2 \right]^{1/2} \right\} / 2E_1 \quad (13)$$

Pour $\nu > 1$ nous avons

$$\begin{aligned} E_1 &= -\varepsilon_1 C_1 \\ E_2 &= (\varepsilon_1 + \varepsilon_2) \left(n C_1 / \bar{U}_1^2 - C_2 \right) + \varepsilon_2 (\varepsilon_1 + \varepsilon_3) \bar{\Delta}_4 \\ E_2' &= (\varepsilon_1 - \varepsilon_2) \left(n C_1 / \bar{U}_1^2 - C_2 \right) + \varepsilon_2 (\varepsilon_1 - \varepsilon_3) \bar{\Delta}_4 \\ E_3 &= \nu C_1 \left(1 / \bar{x}^2 - 1 / \bar{U}_1^2 \right) - \varepsilon_2 \bar{\Delta}_4 \\ \sigma &= \text{sgn}(\xi - 1) \end{aligned} \quad (14)$$

$$\begin{aligned}
C_1 &= (\xi - 1) \left[(\varepsilon_1 + \varepsilon_2) \bar{\Delta}_2 - \varepsilon_3 (\xi - 1) / (\nu - 1) \right] \\
C_2 &= (\xi - 1) \left[(\varepsilon_2 + \varepsilon_3) \bar{\Delta}_3 + \varepsilon_3 \bar{\Delta}_1 / (\nu - 1) \right]
\end{aligned} \tag{15}$$

Et pour $\nu = 1$

$$\begin{aligned}
E_1 &= \varepsilon_1 (\xi - 1) \\
E_2 &= -(\varepsilon_1 + \varepsilon_2) \left[\bar{\Delta}_1 + (\xi - 1) / \bar{U}_1^2 \right] \\
E_2' &= -(\varepsilon_1 - \varepsilon_2) \left[\bar{\Delta}_1 + (\xi - 1) / \bar{U}_1^2 \right] \\
E_3 &= (\xi - 1) \left(1/\bar{x}^2 - 1/\bar{U}_1^2 \right) \\
\sigma &= \text{sgn}(\xi - 1)
\end{aligned} \tag{16}$$

4. Limites loin de la coupure

Ceci constitue la partie originale du mémoire. Lorsque l'on est très loin de la coupure, la puissance modale tend à être confinée dans le cœur. Ceci correspond au paramètre modal du milieu extérieur $W \rightarrow \infty$, c'est-à-dire quand le rayon de gaine $\rightarrow \infty$, mais avec le paramètre modal de gaine qui doit conserver une valeur finie. C'est finalement la même situation que pour la fibre à deux couches où $W \rightarrow \infty$ mais avec le paramètre de cœur qui reste fini. On obtient finalement les équations limites

$$\bar{\eta}_1 \bar{\Delta}_2 - \bar{\Delta}_3 = 0 \quad \text{mode } TE \tag{17}$$

$$\varepsilon_1 \bar{\eta}_1 \bar{\Delta}_2 - \varepsilon_2 \bar{\Delta}_3 = 0 \quad \text{mode } TM \tag{18}$$

puis pour les modes *HE* et *EH*:

$$\bar{\eta}_1 = \frac{\nu}{\bar{x}^2} + \frac{-E_2 \pm \left[(E_2')^2 + 4\varepsilon_1 E_3^2 \right]^{1/2}}{E_1} \quad (19)$$

où

$$\begin{aligned} E_1 &= 2\varepsilon_1 D_1 \\ E_2 &= (\varepsilon_1 + \varepsilon_2) D_2 \\ E_2' &= (\varepsilon_1 - \varepsilon_2) D_2 \\ E_3 &= \nu n_{eff} \left[\left(\frac{1}{\bar{x}^2} - \frac{1}{\bar{U}_1^2} \right) D_1 + \frac{\varepsilon_2}{\bar{U}_2^2} \bar{\Delta}_4 \right] \end{aligned} \quad (20)$$

$$\begin{aligned} D_1 &= \varepsilon_2 \left(\bar{\Delta}_2 - \frac{2\nu(\xi-1)}{\bar{U}_2^2} \right) \bar{\Delta}_2 \\ D_2 &= \frac{\nu}{\bar{U}_1^2} D_1 - \frac{\nu\varepsilon_2}{\bar{U}_2^2} \left[\bar{\Delta}_4 - 2(\xi-1)\bar{\Delta}_3 \right] - \varepsilon_2 \bar{\Delta}_2 \bar{\Delta}_3 \end{aligned} \quad (21)$$

Le choix de signe « + » ou « - » dans les expressions définit respectivement les deux familles de modes hybrides *EH* et *HE*. Finalement, les solutions des équations limites (12) et (17) pour les modes *TE*, (11) et (18) pour les modes *TM* puis (13) et (19) pour les modes hybrides *HE* et *EH* permettent de borner chaque solution des équations aux valeurs propres.

4. Vérifications, calculs numériques

On peut vérifier de plusieurs façons indirectes la validité des équations limites obtenues pour les équations aux valeurs propres à la

coupure puis loin de la coupure. Une première façon est de regarder les «limites» de ces limites quand on passe de la fibre à trois couches à la fibre à deux couches en faisant tendre le rayon de cœur vers le rayon de gaine. On a vérifié que ces limites étaient bien les mêmes que celles données par *Snyder et Love*. Une autre façon est de calculer les indices effectifs d'un mode correspondant à sa coupure et loin de sa coupure puis celui du mode et de vérifier que sa valeur se situe bien entre les deux valeurs précédentes. On a pris comme exemple le cas de la fibre SMF28™ opérant à la longueur d'onde de $1.55\text{ }\mu\text{m}$ avec un facteur de réduction R (réduction homothétique de toutes les dimensions de la fibre) allant de 0.2 à 1. Les trois figures suivantes illustrent ces calculs et l'on peut constater que les courbes des indices effectifs sont bien bornés par les deux courbes correspondant respectivement à la coupure (sauf pour HE_{11} qui n'a pas de coupure) et loin de la coupure.

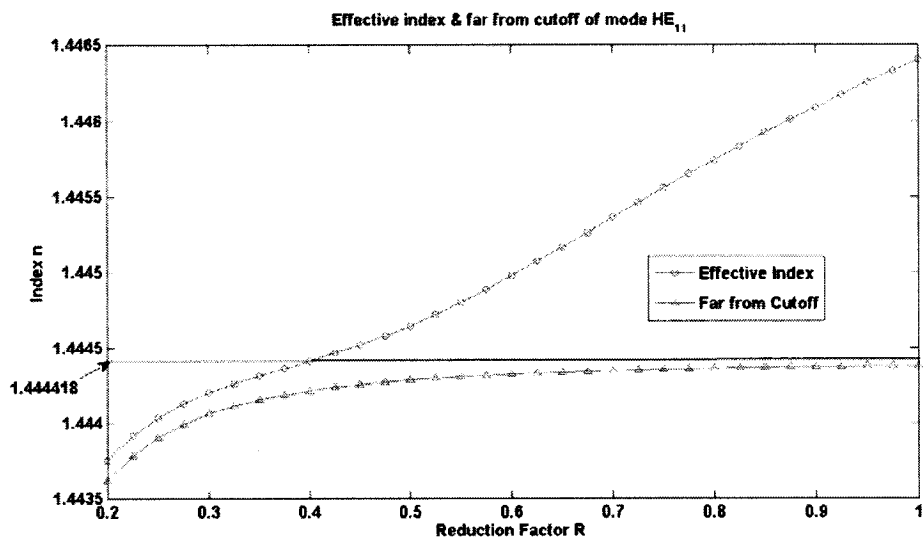


Figure 1 : Indice effectif du mode HE_{11} et sa borne inférieure en fonction de R .

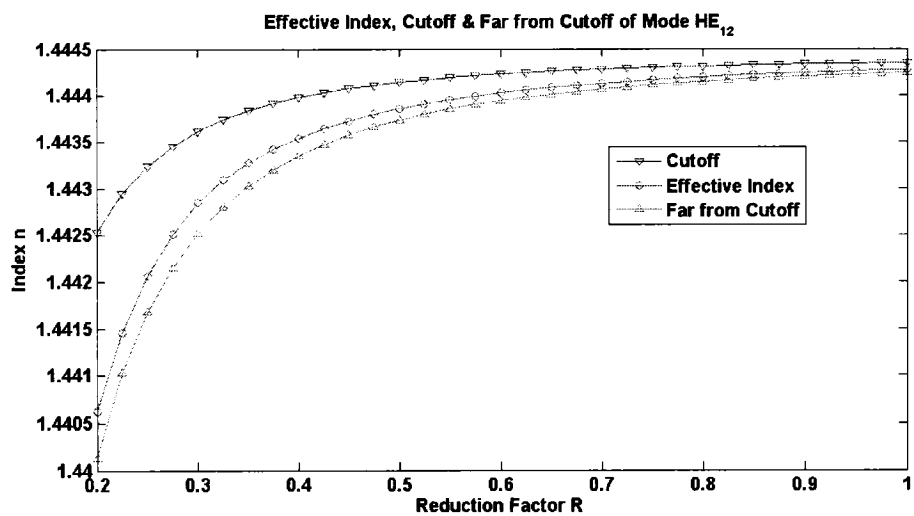


Figure 2 : Indice effectif du mode HE_{12} et ses deux bornes en fonction de R .

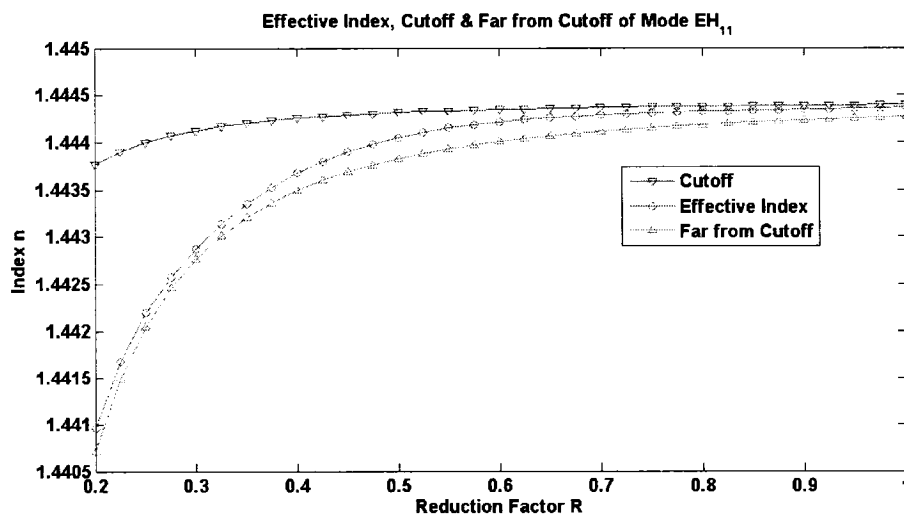


Figure 3 : Indice effectif du mode EH_{11} et ses deux bornes en fonction de R .

5. Conclusion

En conclusion, nous avons utilisé et complété les résultats de *Safaai-Jazi et Yip* en établissant les limites des équations aux valeurs propres loin des coupures. De cette façon, on est maintenant capable de borner chaque solution modale. C'est un moyen efficace de vérifier le numérotage des modes et d'éviter ainsi de sauter accidentellement une des solutions de la série.

Nous avons vérifié que, pour une série de modes (par exemple modes HE_{1m}), nous n'avons pas de chevauchement.

Toutefois, il n'est pas très aisé de calculer les valeurs à la coupure et loin-de-coupure. Nous pensons qu'il est peut-être possible de

borner les “bornes” de façon simple, ce qui éliminerait le numérotage des solutions.

Il reste à généraliser tout ce que nous avons fait pour les trois couches au cas des multicouches, particulièrement les quatre couches où il semblerait que l'équation générale aux valeurs propres peut encore se mettre sous la forme d'une équation quadratique.¹⁶

Table of Contents

Acknowledgments	IV
Summary.....	V
Abstract.....	VIII
Condensé en Français	X
List of Figures	XXVII
List of Tables	XXVIII
List of symbols.....	XXIX

Chapter 1 Introduction.....	1
1.1 Introduction.....	1
1.2 Maxwell's Equation	6
1.2.1 Maxwell's Equation	6
1.2.2 Inhomogeneous Wave Equation.....	8
1.2.3 Boundary Conditions	8
1.2.4 The Mode of Dielectric Waveguides	9
1.2.5 Cylindrical Coordinates	9
1.3 Eigenvalue Equation	10
1.3.1 Ideal Fibre	10
1.3.2 Eigenvalue Equation	11
Chapter 2 Classification of Modes in Two Layer Fibres ..	15
2.1. Introduction.....	15
2.2 Eigenvalue Equation	16
2.2.1 Helmholtz Equation and Solution.....	17
2.2.2 Transverse Modes TE_{0m} and TM_{0m}	24

2.2.3	Hybrid Mode HE_{vm} and EH_{vm}	25
2.3	Value Range of Effective Index	26
2.3.1	Value Range	26
2.3.2	Cutoff Condition	27
2.3.3	Far-from-cutoff Condition	28
2.4	Conclusion	29
Chapter 3 Classification of Modes in Three Layer Fibres33		
3.1	Introduction.....	33
3.2	Eigenvalue Equation	36
3.2.1	Introduction.....	36
3.2.2	Index Profile.....	37
a)	Cladded Fibre.....	37
b)	Dielectric Tube Fibre	37
c)	W -type Fibre.....	38
3.2.3	The Maxwell Equation and Wave Equation	39
3.2.4	Boundary Conditions	40
3.2.5	Eigenvalue Equation of Hybrid mode HE and EH	41
3.2.6	Eigenvalue Equations of Modes TE and TM	57
3.3	Cutoff Conditions.....	57
3.3.1	Cutoff Condition of Mode TE and TM	58
3.3.2	Cutoff Condition of Mode HE and EH	58
3.4	Far-from-cutoff Condition of Mode HE and EH	59
3.4.1	Far-from-cutoff Condition of TE and TM mode.....	60
3.4.2	Far-from-cutoff Condition of HE and EH modes	61
Chapter 4 Verification, Numerical Calculation.....63		
4.1	Transition from three layer to two layer.....	63
4.1.1	Eigenvalue Equation	63
4.1.2	Cutoff Condition	64
4.1.3	Far-from-cutoff Condition	65
4.2	Numerical Calculation of the value range.....	68

4.2.1	Introduction.....	68
4.2.2	Plot of Modes TE and TM	70
4.2.3	Plot of Modes HE	72
4.2.4	Plot of Modes EH	76
4.2.5	Plot of value ranges of modes.....	78
4.3	Discussion.....	78
Chapter 5 Conclusion.....		80
Reference		83

List of Figures

Fig. 1	Propagation of electromagnetic field.....	6
Fig. 2	Conventional step-index fibre.....	16
Fig. 3	Index profile of cladded fibre	37
Fig. 4	Index profile of tube fibre I.....	38
Fig. 5	Index profile of tube fibre II	38
Fig. 6	Index profile of tube fibre III	38
Fig. 7	Index profile of W-type fibre	39
Fig. 8	Plot of effective index, far-from-cutoff condition of mode TE_{01}	71
Fig. 9	Plot of effective index, far-from-cutoff condition of mode TM_{01}	71
Fig. 10	Plot of effective index, far-from-cutoff condition of mode HE_{11}	72
Fig. 11	Extended plot of mode HE_{11}	73
Fig. 12	Plot of effective index, cutoff and far-from cutoff conditions of mode HE_{12}	73
Fig. 13	Extended plot of mode HE_{12}	74
Fig. 14	Plot of effective index, cutoff and far-from-cutoff conditions of mode HE_{21}	75
Fig. 15	Plot of effective index, cutoff and far-from-cutoff conditions of mode HE_{22}	75
Fig. 16	Plot of effective index, cutoff and far-from-cutoff condition of mode EH_{11}	76
Fig. 17	Extended plot of mode EH_{11}	76
Fig. 18	Plot of effective index, cutoff and far-from cutoff conditions of mode EH_{12}	77
Fig. 19	Extended plot of mode EH_{12}	77
Fig. 20	Plot of value ranges of modes EH_{11} and EH_{12}	78

List of Tables

Table 1	Cutoff of two layer fibre	28
Table 2	The far-from-cutoff of two layer fibre.....	29
Table 3	The generalized function	42
Table 4	The small argument approximation.....	58
Table 5	The definition of fibre $SMF-28^{TM}$	70

List of symbols

\vec{J} : Density of current

σ : Density of charge

ω : Angular frequency

k : Wave number

λ : Wave length

n : Index of medium

ε : Dielectric permittivity

μ : Magnetic permittivity

\vec{E} : Electric field

\vec{H} : Magnetic field

β : Propagation constant along the axe

U, W, V : Modal parameters and normalized frequency

ρ : Radius of the fibre

CHAPTER 1

INTRODUCTION

1.1 Introduction

Due to its physical and chemical stability, not subject to electromagnetic interference, high transmission bandwidth and low loss, optical fibre has been regarded as the ideal medium in which communication signals are transmitted from one location to another in the form of light guided through thin fibre of glass or plastic. Optical fibre is the most promising optical waveguide used in optical communication and optical information processing systems. It consists of a core having uniform or graded refractive index and a cladding with a smaller refractive index. The propagating of light in the optical fibre can be described as the transmission of an electromagnetic wave in the optical waveguide.^{1 2 3 4}

Classification of mode in cylindrical dielectric waveguides has always been important to the investigation of modes in optical fibre. Except the axial symmetric transverse mode, TE_{0m} and TM_{0m} modes, all the modes are hybrid modes, HE_{vm} or EH_{vm} modes.

When modes in optical fibre are being investigated, a primary assumption is that the cladding radius extends to infinity, or the ratio of cladding radius to the core radius is big enough. Then the optical fibre is then regarded as a two layer dielectric waveguide, and the eigenvalue equation, the cutoff frequency and the far-from-cutoff frequency of TE , TM , even HE and EH modes can be easily obtained.^{5 6 7} The eigenvalue of each mode of a two layer dielectric waveguide varies between the value range formed by the cutoff and the far-from-cutoff condition given by *Snyder and Love*,⁷ which will be discussed later in this paper.

In order to distinguish between EH and HE modes, *Snitzer*⁵ proposed an amplitude coefficient ratio P , which is the ratio of amplitude of E_z and H_z , to designate the hybrid modes of the dielectric rod. $P = +1$ designates EH mode and $P = -1$ designates HE mode.

In practice, the sign of the roots of the quadratic eigenvalue equation is employed to classify the EH and HE modes.^{8, 9}

If the ratio is not big enough, the structure of optical fibre with step-index profile will become a three layer dielectric waveguide, or three layer cladded fibre structure. Depending on the index profiles of the three layer structures, it can be classified into cladded fibre, tubular and W -type structure.

The complexity of cylindrical dielectric waveguides brings the complexity of modal classification. For example, *Snitzer's*⁵ scheme was revealed not to be proper to classify the hybrid mode in cladded fibre by *A. Safaai-Jazi and al.*^{8 9} Some other articles^{10 11 12 13} proposed the methods of eigenvalue equation of modes to classify the hybrid modes in various structures of three layer or multilayer cylindrical dielectric waveguides, like dielectric rode and dielectric tube. The two sets of roots of a quadratic equation could be used to designate the hybrid modes, *HE* and *EH* modes in arbitrary three layer structures. The set of roots which might give the zero cutoff frequency corresponding to the dominant *HE*₁₁ designates the *HE* modes, whereas the other set of roots designates *EH* mode. But none of the above-mentioned methods can apply to all the structures. To find a global scheme used to designate hybrid modes in all the structures of cylindrical dielectric waveguides. *Safaai-Jazi et al*^{8 9} obtained the eigenvalue equation for the three layer structures.

Out of various important aspects of dielectric waveguides, cutoff conditions play a major role in the understanding and design of such structures and the selection of operation wavelength. Some of the above-mentioned articles describe the cutoff conditions of two and three layer dielectric waveguides.¹⁴ The far-from-cutoff condition is hardly mentioned and it is believed that it is just as important as the cutoff

condition. Because the cutoff and the far-from-cutoff conditions form a range, in which the effective index of mode varies, it is helpful to characterize the modes of dielectric waveguides more precisely and efficiently.

Compared with the two layer structure, the derivation of the cutoff and the far-from-cutoff expressions should be very complicated. *A. Safaai-Jazi and Yip*^{8 9} and *Achint Kapoor and G. S. Singh*¹⁴ derived separate eigenvalue equations for *HE* and *EH* modes in three layer dielectric waveguides.

The global scheme of *A. Safaai-Jazi and Yip*^{8 9} is employed to conduct the mode designation and analysis. The purpose of this thesis is to specify the effective index range bounded by the cutoff and the far-from-cutoff conditions of modes in three layer structures with the aid of the eigenvalue equation method.

Because the transverse components of the fields can be expressed in terms of the longitudinal components, the vector wave equation becomes two identical partial differential equations of longitudinal components E_z and H_z . The eigenvalue equation can be obtained through the continuous conditions of longitudinal and tangential components at one interface. By setting the effective indices of modes tend to the indices

of two adjacent media, the cutoff and the far-from-cutoff conditions occur. Then the cutoff and the far-from-cutoff expressions could be derived. This is the eigenvalue equation method used widely in two layer cylindrical waveguides.

Similarly, in three layer structures, the effective indices of guided modes could be investigated by determining the two boundaries of the range of modal parameters using the eigenvalue equation method. Since there are two different interfaces in three layer structures, the tangential and longitudinal components of the fields have to be continuous at these two interfaces. An 8x8 matrix will be obtained to let longitudinal and tangential components to comply with the boundary conditions. The determinant of the 8x8 matrix must vanish in order to have a non-trivial solution of the coefficients. Then a quadratic equation of the propagation constant will be obtained, which is called the eigenvalue equation and has two groups of roots, corresponding to the modes HE_{vm} and EH_{vm} .

Three layer structures have 5 or more useful combinations of index profiles; it is extremely difficult to find an appropriate analytic eigenvalue equation to define all the three layer dielectric waveguides. Compared with the two layer structure, the derivation of the eigenvalue equation and the cutoff and the far-from-cutoff conditions is very

complicated. Until now, only *A. Safaai-Jazi and Yip's*^{8 9} global analytic expressions of eigenvalue equation are applicable to some of the most popular three layer structures, like cladded fibre, tubular and *W*-type structure. *Achint Kapoor and G.S. Singh*¹⁴ made a small modification to *A. Safaai-Jazi and Yip's*^{8 9} method.

1.2 Maxwell's Equation

1.2.1 Maxwell's Equation

Light is an electromagnetic wave phenomenon described by the same theoretical principles that govern all forms of electromagnetic radiation. Light propagation in the optical fibre can be described as electromagnetic wave propagation in a circular dielectric waveguide. The basic principles of the theory—Maxwell's equations—are summarized in this section.

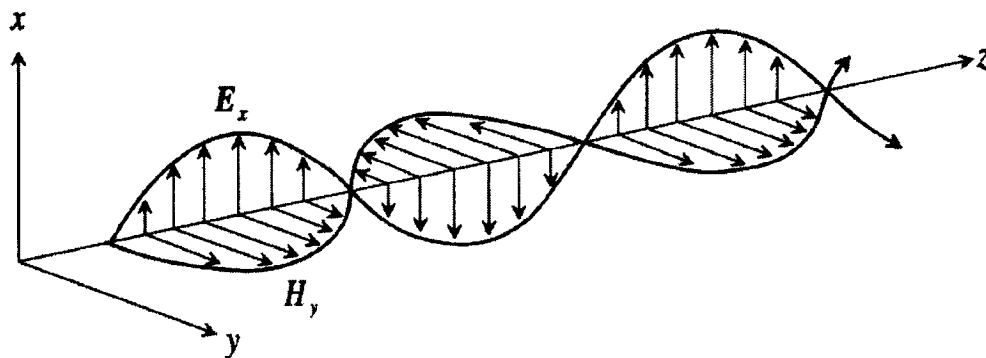


Fig. 1 Propagation of electromagnetic field

An electromagnetic field is described as two related vector fields: the electric field $\vec{E}(\vec{r}, t)$ and the magnetic field $\vec{H}(\vec{r}, t)$. With the existence of the source point, the electric and magnetic fields satisfy the following partial differential equations—Maxwell's equations:

$$\vec{\nabla} \times \vec{E} = -\frac{\partial \vec{B}}{\partial t} \quad (3.1)$$

$$\vec{\nabla} \times \vec{H} = \frac{\partial \vec{D}}{\partial t} + \vec{J} \quad (3.2)$$

$$\vec{\nabla} \cdot \vec{B} = 0 \quad (3.3)$$

$$\vec{\nabla} \cdot \vec{D} = \rho \quad (3.4)$$

where

$$\begin{aligned} \vec{D} &= \epsilon \vec{E} \\ \vec{B} &= \mu \vec{H} \\ \epsilon &= \epsilon_0 \epsilon_r \\ \mu &= \mu_0 \mu_r \end{aligned} \quad (3.5)$$

The $\vec{E}, \vec{H}, \vec{D}, \vec{B}$ are the electric field, the magnetic field, the electric flux density and the magnetic flux density respectively. The $\epsilon_0, \mu_0, \epsilon_r, \mu_r$ are the permittivity and permeability of a vacuum and the relative permittivity and permeability of the electric waveguide. \vec{J} is the current density and ρ is the charge density.

In the source free region, \vec{J} and ρ are equal to zero, and the

relative permeability is equal to the relative permeability. The Maxwell's equations (3.1)—(3.4) are simplified as follows:

$$\vec{\nabla} \times \vec{E} = -\mu_0 \frac{\partial \vec{H}}{\partial t} \quad (3.6)$$

$$\vec{\nabla} \times \vec{H} = \varepsilon \frac{\partial \vec{E}}{\partial t} \quad (3.7)$$

$$\vec{\nabla} \cdot \vec{H} = 0 \quad (3.8)$$

$$\vec{\nabla} \cdot \varepsilon \vec{E} = 0 \quad (3.9)$$

1.2.2 Inhomogeneous Wave Equation

Combining with some mathematical transformations, the above Maxwell's equations (3.6)—(3.9) could be changed into the following inhomogeneous vector wave equation.⁷

$$\begin{cases} \left(\vec{\nabla}^2 + k^2 n^2 \right) \vec{E} = -\vec{\nabla} \left(\vec{E} \cdot \vec{\nabla} \ln n^2 \right) - i \sqrt{\frac{\mu_0}{\varepsilon_0}} \left\{ k \vec{J} + \frac{1}{k} \vec{\nabla} \left(\frac{\vec{\nabla} \cdot \vec{J}}{n^2} \right) \right\} \\ \left(\vec{\nabla}^2 + k^2 n^2 \right) \vec{H} = \left(\vec{\nabla} \times \vec{H} \right) \times \vec{\nabla} \ln n^2 - \vec{\nabla} \times \vec{J} - \vec{J} \times \vec{\nabla} \ln n^2 \end{cases} \quad (3.10)$$

where k is wave number in vacuum $k = 2\pi/\lambda_0$

1.2.3 Boundary Conditions

The electric and magnetic field should satisfy the boundary

conditions.⁷

The continuity of normal component $\hat{n} \cdot (n^2 \vec{E})$ et $\hat{n} \cdot (\vec{H})$

The continuity of tangential component $\hat{n} \times \vec{E}$ et $\hat{n} \times \vec{H}$

1.2.4 The Mode of Dielectric Waveguides

The electromagnetic field, i.e. the light propagating in the optical fibre, exists in the form of a bound mode. The electromagnetic field in the optical fibre can be decomposed into two series of the bound mode of a waveguide.

The best way to investigate the optical waveguide is to study the fundamental properties of modes of circular optical waveguides. The vector fields of these modes are the solutions of *Maxwell's* homogeneous vector wave equation subject to boundary conditions.

1.2.5 Cylindrical Coordinates

Instead of the Cartesian coordinate utilized in the investigation of slab waveguide, the cylindrical coordinate system (r, ϕ, z) , with the z-axis coinciding with the axis of the dielectric structure, is employed for the mode analysis. With the assumption of the translational invariance and the

t -dependence of field in optical fibre, the term $\exp[i(\beta z - \omega t)]$ can be separated from the expressions of field and dropped in later deduction. In the cylindrical coordinate, the field components could be expressed as:

$$\begin{aligned}\bar{E}(r, \phi, z) &= \bar{e}(r, \phi) e^{i\beta z} \\ \bar{e}(r, \phi) &= \bar{e}_r + \hat{z} e_z = \hat{r} e_r + \hat{\phi} e_\phi + \hat{z} e_z\end{aligned}\tag{3.11}$$

and

$$\begin{aligned}\bar{H}(r, \phi, z) &= \bar{h}(r, \phi) e^{i\beta z} \\ \bar{h}(r, \phi) &= \bar{h}_r + \hat{z} h_z = \hat{r} h_r + \hat{\phi} h_\phi + \hat{z} h_z\end{aligned}\tag{3.12}$$

The $\bar{e}(r, \phi)$ and $\bar{h}(r, \phi)$ are invariant along z . And the scalar Laplacian is rewritten for a cylindrical coordinate system as follows:

$$\begin{aligned}\nabla^2 &= \nabla_r^2 + \frac{\partial^2}{\partial z^2} = \nabla_r^2 - \beta^2 \\ &= \frac{\partial^2}{\partial r^2} + \frac{1}{r} \frac{\partial}{\partial r} + \frac{1}{r^2} \frac{\partial^2}{\partial \phi^2} + \frac{\partial^2}{\partial z^2} \\ &= \frac{\partial^2}{\partial r^2} + \frac{1}{r} \frac{\partial}{\partial r} + \frac{1}{r^2} \frac{\partial^2}{\partial \phi^2} - \beta^2\end{aligned}\tag{3.13}$$

The operator ∇_r^2 is the scalar transversal Laplacian operator.

$$\nabla_r^2 = \frac{1}{r} \frac{\partial}{\partial r} \left(r \frac{\partial}{\partial r} \right) + \frac{1}{r^2} \frac{\partial^2}{\partial \phi^2} = \frac{\partial^2}{\partial r^2} + \frac{1}{r} \frac{\partial}{\partial r} + \frac{1}{r^2} \frac{\partial^2}{\partial \phi^2}\tag{3.14}$$

1.3 Eigenvalue Equation

1.3.1 Ideal Fibre

A typical fibre is considered as an infinitely long cylindrical two layer dielectric structure, consisting of core with a radius ρ and has a uniform refractive index n_1 or n_c , which is slightly higher than the refractive index of the cladding n_2 or n_g . The ideal fibre to be discussed in our future work is assumed to be a non-absorbing, ideal dielectric structure, source free, with perfect circular on the cross section and uniform along its axis.

1.3.2 Eigenvalue Equation

Assuming that the waveguide is an ideal optical fibre, non-absorbing and source free, then the homogeneous vector equation (3.10) can be rewritten as:

$$\begin{cases} (\bar{\nabla}^2 + k^2 n^2) \vec{E} = -\bar{\nabla} (\vec{E} \cdot \bar{\nabla} \ln n^2) \\ (\bar{\nabla}^2 + k^2 n^2) \vec{H} = (\bar{\nabla} \times \vec{H}) \times \bar{\nabla} \ln n^2 \end{cases} \quad (3.15)$$

Due to the invariance of \vec{e} and \vec{h} along z , the vector Gradient operators $\bar{\nabla}$ and Laplacian operators $\bar{\nabla}^2$ in equation (3.15) can be rewritten as:

$$\bar{\nabla} = \bar{\nabla}_t + \hat{z} \frac{\partial}{\partial z} \quad (3.16)$$

where the $\bar{\nabla}_t$ is the transversal Gradient operator

$$\bar{\nabla}^2 \bar{A} = \bar{\nabla}_t^2 \bar{A} + \frac{\partial^2 \bar{A}}{\partial z^2} = \bar{\nabla}_t^2 \bar{A} - \beta^2 \bar{A} \quad (3.17)$$

where the $\bar{\nabla}_t^2$ is vector transversal Laplacian operator.

Substituting the equation(3.11), (3.12), (3.16) and (3.17) into the equation (3.15), the vector wave equation can be reduced to a homogeneous vector wave equation,⁷

$$\begin{cases} (\bar{\nabla}_t^2 + k^2 n^2 - \beta^2) \bar{e} = -(\bar{\nabla}_t + i\beta \hat{z})(\bar{e}_t \cdot \bar{\nabla}_t \ln n^2) \\ (\bar{\nabla}_t^2 + k^2 n^2 - \beta^2) \bar{h} = \{(\bar{\nabla}_t + i\beta \hat{z}) \times \bar{h}\} \times \bar{\nabla}_t \ln n^2 \end{cases} \quad (3.18)$$

β is called the axial propagation constant or eigenvalue of the mode of the waveguide. Generally each mode has a unique value of β_j .

Through the above boundary conditions, the homogeneous vector equations can be rewritten as equation groups of variable β . This equation of eigenvalue β is called the eigenvalue equation of a waveguide or the characteristic equation of a waveguide.

Because the field's transverse component can be expressed with the field's longitudinal components, it's only necessary to solve the longitudinal component e_z and h_z .

The transverse and axial component can be expressed in separated form because of the cylindrical symmetry and z -dependence, or translational invariance, of the waveguide. All fields contain the implicit

time dependence $\exp(-i\omega t)$, where ω is the angular frequency.

Assuming the discussed optical fibre has step-index profile, the term of $\vec{\nabla} \ln n^2$ in the equation (3.18) is vanished

$$\begin{cases} (\vec{\nabla}_t^2 + k^2 n^2 - \beta^2) \vec{e} = 0 \\ (\vec{\nabla}_t^2 + k^2 n^2 - \beta^2) \vec{h} = 0 \end{cases} \quad (3.19)$$

All three components of the electric field and magnetic field in the Cartesian coordinates satisfy the Helmholtz equation(3.19), but only the z-component of electric field and magnetic field in the cylindrical coordinates satisfies the Helmholtz equation(3.19). The components of electric and magnetic fields can be expressed as:

$$\begin{aligned} \vec{e}(r, \phi) &= \vec{e}_t + \hat{z} e_z = \hat{r} e_r(r, \phi) + \hat{\phi} e_\phi(r, \phi) + \hat{z} e_z(r, \phi) \\ \vec{h}(r, \phi) &= \vec{h}_t + \hat{z} h_z = \hat{r} h_r(r, \phi) + \hat{\phi} h_\phi(r, \phi) + \hat{z} h_z(r, \phi) \end{aligned} \quad (3.20)$$

And then substituting equation(3.13), (3.14) and (3.20) into equation(3.19), a new differential coupled equation of longitudinal field components will be obtained:

$$\begin{cases} \nabla_t^2 e_z + \{n^2 k^2 - \beta^2\} e_z = 0 \\ \nabla_t^2 h_z + \{n^2 k^2 - \beta^2\} h_z = 0 \end{cases} \quad (3.21)$$

If the longitudinal and temporal variations are combined, the modal fields vary as $\exp[i(\beta_j z - \omega t)]$, and, consequently, each mode

propagates along the waveguides with phase velocity $v_j = \omega / \beta_j$.

Alternatively, the electric and magnetic fields can be generated by solving the same equations in regions where the profile is continuous, and matching any discontinuities through the appropriate boundary conditions of *Maxwell's* equations. In either case, the formulation leads to a consistent condition for determining the modal propagation constants β , i.e. an eigenvalue equation.

CHAPTER 2

CLASSIFICATION OF MODES IN TWO LAYER FIBRES

2.1. Introduction

The typical optical fibre consists of a core having uniform or graded refractive index and a cladding with a smaller refractive index. The small difference of the index of core and cladding at the interface makes some of the propagating light in the core satisfy continually the total internal reflection condition at the interface of core and cladding. The optical fibre is actually a circular dielectric waveguide which permits the light signals to propagate along the fibre.

The optical fibre is classified into two primary kinds according to its core index profile, namely, step-index and graded profile. To find the global scheme of modal classification, only step-index profile fibre will be discussed.

The classification of modes in two layer structures will be presented before the more complicated discussion of three layer structures.

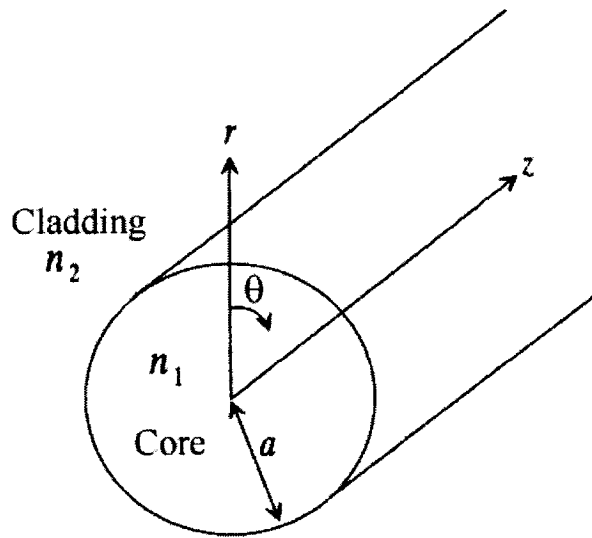


Fig. 2 Conventional step-index fibre

A typical two layer fibre is considered as an infinitely long cylindrical two layer dielectric structure, consisting of core of a radius ρ and having a uniform refractive index n_1 or n_c , which is slightly higher than the refractive index of the cladding n_2 or n_g and is assumed to extend to infinity in the radial direction.

The ideal fibre to be discussed in the future work will be viewed as a non-absorbing, ideal dielectric structure, source free and perfectly circular on the cross section and uniform along its axis.

2.2 Eigenvalue Equation

2.2.1 Helmholtz Equation and Solution

As mentioned in Chapter 1, the term of $\bar{\nabla} \ln n^2$ in the vector wave equation has disappeared in the case of step-index fibre. The electromagnetic fields are the solutions of the Helmholtz equation subject to boundary conditions.

In the cylindrical coordinate systems, the scalar wave equation (3.21) is rewritten as

$$(\nabla_t^2 + k^2 n^2 - \beta^2) \Psi = 0 \quad (2.1)$$

where Ψ is the longitudinal components of electric or magnetic fields. ∇_t^2 is the transverse Laplacian operator defined by equation (3.14), $k_0 = 2\pi/\lambda$ is the free space wave number, and n is the refractive index of the medium discussed.

With the following equations, the field's transverse component could be expressed with the field's longitudinal components; therefore it is only necessary to solve the longitudinal component e_z and h_z .

$$\begin{aligned} \vec{e}_y &= \frac{i}{n^2 k^2 - \beta_j^2} \left\{ \beta_j \bar{\nabla}_t e_{zj} - \left(\frac{\mu_0}{\epsilon_0} \right)^{1/2} k \hat{z} \times \bar{\nabla}_t h_z \right\} \\ \vec{h}_y &= \frac{i}{n^2 k^2 - \beta_j^2} \left\{ \beta_j \bar{\nabla}_t h_{zj} + \left(\frac{\epsilon_0}{\mu_0} \right)^{1/2} k n^2 \hat{z} \times \bar{\nabla}_t e_z \right\} \end{aligned} \quad (2.2)$$

All fields contain the implicit time dependence $\exp(-i\omega t)$, where

ω is the angular frequency.

Considering the axial symmetry of the function Ψ , we could apply the method of separate variables, and then the function of $\Psi(r, \phi)$ is given by:

$$\Psi(r, \phi) = R(r)\Phi(\phi) \quad (2.3)$$

Substituting above expression (2.3) into Helmholtz equation (2.1), we get

$$\frac{1}{R(r)} \left[\frac{\partial^2 R(r)}{\partial r^2} + \frac{1}{r} \frac{\partial R(r)}{\partial r} \right] + \frac{1}{r^2} \frac{1}{\Phi(\phi)} \frac{\partial^2 \Phi(\phi)}{\partial \phi^2} + k_0^2 (n^2 - n_{eff}^2) = 0 \quad (2.4)$$

Therefore

$$\frac{r^2}{R(r)} \left[\frac{\partial^2 R(r)}{\partial r^2} + \frac{1}{r} \frac{\partial R(r)}{\partial r} \right] + r^2 k_0^2 (n^2 - n_{eff}^2) = - \frac{1}{\Phi(\phi)} \frac{\partial^2 \Phi(\phi)}{\partial \phi^2} \quad (2.5)$$

Since each hand of this equation is a function of only the one variable respectively, both sides have to be constant to keep the equation true. Thus, we obtain

$$\frac{r^2}{\Psi(r)} \left[\frac{d^2 \Psi(r)}{dr^2} + \frac{1}{r} \frac{d\Psi(r)}{dr} \right] + r^2 k_0^2 (n^2 - n_{eff}^2) = - \frac{1}{\Phi(\phi)} \frac{d^2 \Phi(\phi)}{d\phi^2} = \nu^2 \quad (2.6)$$

ν is a separation constant, and the equation (2.6) resolves into the following two ordinary differential equations:

$$\frac{d^2 R(r)}{dr^2} + \frac{1}{r} \frac{dR(r)}{dr} + \left[k_0^2 (n^2 - n_{eff}^2) - \frac{\nu^2}{r^2} \right] R(r) = 0 \quad (2.7)$$

$$\frac{d^2 \Phi(\phi)}{d\phi^2} + \nu^2 \Phi(\phi) = 0 \quad (2.8)$$

The solution to the equation of angular variable $\Phi(\phi)$ has the same value after a rotation of 2π in the cross section, i.e. $R(r, \phi) = R(r, \phi + 2\pi)$, it is necessary that ν be an integer. Each $\cos(\nu\phi)$ and $\sin(\nu\phi)$ could be used in the expressions of fields as their linear combinations. Then ϕ -dependence of the field could be written simply as:

$$\Phi(\phi) = \begin{cases} \cos(\nu\phi) \\ \sin(\nu\phi) \end{cases} \quad (2.9)$$

where ν is a positive integer greater than or equal to zero. Two functional bases are chosen to construct the field function.

$$f_\nu(\phi) = \begin{cases} \cos(\nu\phi) \\ \sin(\nu\phi) \end{cases} \quad (2.10)$$

$$g_\nu(\phi) = \begin{cases} -\sin(\nu\phi) \\ \cos(\nu\phi) \end{cases} \quad (2.11)$$

Defining waveguide parameters,

$$U = k\rho\sqrt{n_c^2 - n_{eff}^2} \quad (2.12)$$

and

$$W = k\rho\sqrt{n_{eff}^2 - n_g^2} \quad (2.13)$$

The equation of radial variable could be written as:

$$\frac{d^2 R(r)}{dr^2} + \frac{1}{r} \frac{dR(r)}{dr} + \left(\frac{U^2}{\rho^2} - \frac{\nu^2}{r^2} \right) R(r) = 0 \quad \text{in the core} \quad (2.14)$$

$$\frac{d^2 \Psi(r)}{dr^2} + \frac{1}{r} \frac{d\Psi(r)}{dr} - \left(\frac{W^2}{\rho^2} + \frac{\nu^2}{r^2} \right) \Psi(r) = 0 \quad \text{in the cladding} \quad (2.15)$$

where n_c and n_g are the indices of core and exterior media respectively.

Equation (2.14) is the first kind of Bessel differential equation which has the following solution form

$$R(r) = A_1 J_\nu \left(U \frac{r}{\rho} \right) + A_2 Y_\nu \left(U \frac{r}{\rho} \right) \quad (2.16)$$

Equation (2.15) is the second kind of Bessel differential equation which has the following solution form

$$R(r) = A_3 I_\nu \left(W \frac{r}{\rho} \right) + A_4 K_\nu \left(W \frac{r}{\rho} \right) \quad (2.17)$$

where J_ν is the first kind of Bessel function, Y_ν is the second kind of Bessel function, I_ν is the first kind of modified Bessel function and K_ν is the second kind of modified Bessel function. A_1, A_2, A_3, A_4 are coefficients.

However, the two layer structures, solutions of the form (2.16) and (2.17) can be simplified. In the core, the solution Y_ν should be discarded because Y_ν diverge as $r = 0$. In the cladding, the solution I_ν

should be discarded either because I_ν diverge as $r \rightarrow \infty$. A_2 and A_3 has to be zero to reject these two terms in equation (2.16) and equation (2.17).

Thus, the function $\Psi(r, \phi)$ has the form as follow:

$$\Psi(r, \phi) = \begin{cases} J_\nu \left(U \frac{r}{\rho} \right) f_\nu(\phi) / J_\nu(U) & 0 \leq r \leq \rho \\ K_\nu \left(W \frac{r}{\rho} \right) f_\nu(\phi) / K_\nu(W) & r > \rho \end{cases} \quad (2.18)$$

or

$$\Psi(r, \phi) = \begin{cases} J_\nu \left(U \frac{r}{\rho} \right) g_\nu(\phi) / J_\nu(U) & 0 \leq r \leq \rho \\ K_\nu \left(W \frac{r}{\rho} \right) g_\nu(\phi) / K_\nu(W) & r > \rho \end{cases} \quad (2.19)$$

Based on function $\Psi(r, \phi)$, the field's longitudinal components e_z and h_z can be expressed as follows:

$$e_z(r, \phi) = f_\nu(\phi) \begin{cases} A_1 J_\nu \left(U \frac{r}{\rho} \right) & 0 \leq r \leq \rho \\ A_2 K_\nu \left(W \frac{r}{\rho} \right) & r > \rho \end{cases} \quad (2.20)$$

and

$$h_z(r, \phi) = g_\nu(\phi) \begin{cases} B_1 J_\nu \left(U \frac{r}{\rho} \right) & 0 \leq r \leq \rho \\ B_2 K_\nu \left(W \frac{r}{\rho} \right) & r > \rho \end{cases} \quad (2.21)$$

Since the boundary condition requires that the tangential

components of electric and magnetic field are equal at the interfaces between adjacent media, the boundary conditions are expressed as:

$$\begin{aligned} e_z(\rho-0) &= e_z(\rho+0) \\ e_\phi(\rho-0) &= e_\phi(\rho+0) \end{aligned} \quad (2.22)$$

Thus we finally obtain the field's longitudinal components as:

$$e_z(r, \phi) = A f_v(\phi) \begin{cases} J_v\left(U r / \rho\right) / J_v(U) & 0 \leq r \leq \rho \\ K_v\left(W r / \rho\right) / K_v(W) & r > \rho \end{cases} \quad (2.23)$$

and

$$h_z(r, \phi) = B g_v(\phi) \begin{cases} J_v\left(U r / \rho\right) / J_v(U) & 0 \leq r \leq \rho \\ K_v\left(W r / \rho\right) / K_v(W) & r > \rho \end{cases} \quad (2.24)$$

where A and B are coefficients.

With the obtained longitudinal components, we can get the other components of electric and magnetic fields, i.e. radial and angular ones. We summarize the fields of two layer cylindrical dielectric waveguides in core and cladding region respectively.

At the interface of core and cladding, only the longitudinal and angular components satisfy the continuity conditions. The angular component is given as follow:

$$\begin{aligned}
e_\phi &= g_v(\phi) \frac{i\rho^2}{U^2} \left\{ A\nu \frac{\beta}{r} \frac{J_v(U r/\rho)}{J_v(U)} - B \sqrt{\frac{\mu_0}{\varepsilon_0}} k \frac{U}{\rho} \frac{J'_v(U r/\rho)}{J_v(U)} \right\} & 0 \leq r \leq \rho \\
e_\phi &= g_v(\phi) \frac{i\rho^2}{W^2} \left\{ A\nu \frac{\beta}{r} \frac{K_v(W r/\rho)}{K_v(W)} - B \sqrt{\frac{\mu_0}{\varepsilon_0}} k \frac{U}{\rho} \frac{J'_v(W r/\rho)}{J_v(W)} \right\} & r > \rho
\end{aligned} \tag{2.25}$$

and

$$\begin{aligned}
h_\phi &= \frac{i\rho^2}{U^2} f_v(\phi) \left\{ -\nu B \frac{\beta}{r} \frac{J_v(U r/\rho)}{J_v(U)} + A \sqrt{\frac{\varepsilon_0}{\mu_0}} k n^2 \frac{U}{\rho} \frac{J'_v(U r/\rho)}{J_v(U)} \right\} & 0 \leq r \leq \rho \\
h_\phi &= \frac{i\rho^2}{U^2} f_v(\phi) \left\{ -\nu B \frac{\beta}{r} \frac{K_v(W r/\rho)}{K_v(W)} + A \sqrt{\frac{\varepsilon_0}{\mu_0}} k n^2 \frac{W}{\rho} \frac{K'_v(W r/\rho)}{K_v(W)} \right\} & r > \rho
\end{aligned} \tag{2.26}$$

Substituting the continuity conditions of angular components of electric and magnetic fields at the interface of core and cladding, two equations of coefficient A and B will be obtained. This equation group could be rewritten as a matrix as follow:

$$\begin{bmatrix}
\nu\beta \left(\frac{V}{UW} \right)^2 & -\sqrt{\frac{\mu_0}{\varepsilon_0}} k \left[\frac{J'_v(U)}{UJ_v(U)} + \frac{K'_v(W)}{WK_v(W)} \right] \\
\sqrt{\frac{\varepsilon_0}{\mu_0}} k \left(n_c^2 \frac{J'_v(U)}{UJ_v(U)} + n_g^2 \frac{K'_v(W)}{WK_v(W)} \right) & -\nu\beta \left(\frac{1}{UW} \right)^2
\end{bmatrix} \begin{bmatrix} A \\ B \end{bmatrix} = 0 \tag{2.27}$$

As the coefficients A and B have nontrivial solutions, the determinant of the left matrix has to be zero. Then, an equation will be obtained as follow⁷:

$$(\nu n_{\text{eff}})^2 \left(\frac{V}{UW} \right)^4 = \left[\frac{J'_\nu(U)}{UJ_\nu(U)} + \frac{K'_\nu(W)}{WK_\nu(W)} \right] \left(n_c^2 \frac{J'_\nu(U)}{UJ_\nu(U)} + n_g^2 \frac{K'_\nu(W)}{WK_\nu(W)} \right) \quad (2.28)$$

This is the eigenvalue equation for the hybrid mode (i.e. $e_z \neq 0$ and $h_z \neq 0$). U and W are functions of the effective index, so the primary variable of this eigenvalue equation is the effective index of mode in the optical waveguide n_{eff} , which depends on the parameters ν , n_c , n_g and V . This equation has some discrete solutions which correspond to the guide modes in the waveguide.

2.2.2 Transverse Modes TE_{0m} and TM_{0m}

As $\nu=0$, one of $f_\nu(\phi)$ and $g_\nu(\phi)$ is equal to zero, the other one is equal to 1. The corresponding modes with circular symmetric fields in cylindrical dielectric waveguides are transverse electric (TE) which corresponds to $E_z = 0$, and transverse magnetic (TM) which corresponds to $H_z = 0$ in the course of their propagation.

The eigenvalue equations of the transverse modes ($\nu=0$) will be as follows:

$$\left[\frac{J'_0(U)}{UJ_0(U)} + \frac{K'_0(W)}{WK_0(W)} \right] \left(n_c^2 \frac{J'_0(U)}{UJ_0(U)} + n_g^2 \frac{K'_0(W)}{WK_0(W)} \right) = 0 \quad (2.29)$$

According to the definition of Bessel function,¹⁵ we have

$J'_0(U) = -J_1(U)$ and $K'_0(W) = -K_1(W)$, the eigenvalue equation of transverse mode is rewritten as

$$\left[\frac{J_1(U)}{UJ_0(U)} + \frac{K_1(W)}{WK_0(W)} \right] \left(n_c^2 \frac{J_1(U)}{UJ_0(U)} + n_g^2 \frac{K_1(W)}{WK_0(W)} \right) = 0 \quad (2.30)$$

This equation splits into two independent eigenvalue equations corresponding to transverse modes TE and TM . With the help of the continuity conditions of $\hat{n} \cdot (n^2 \vec{E})$ et $\hat{n} \cdot (\vec{H})$, we could classify these two equations as follow

The eigenvalue equation of mode TE_{0m}

$$\frac{J_1(U)}{UJ_0(U)} + \frac{K_1(W)}{WK_0(W)} = 0 \quad (2.31)$$

The eigenvalue equation of mode TM_{0m}

$$n_c^2 \frac{J_1(U)}{UJ_0(U)} + n_g^2 \frac{K_1(W)}{WK_0(W)} = 0 \quad (2.32)$$

2.2.3 Hybrid Mode $HE_{\nu m}$ and $EH_{\nu m}$

As $\nu \geq 1$, the situation of $f_\nu(\phi)$ and $g_\nu(\phi)$ equal to zero or one will not appear. Thus $\nu \geq 1$ corresponds to the non-symmetric modes which are hybrid ones; they are superposition of TE and TM mode fields, due to the fact that both *Debye* potentials E_z and H_z are needed to construct angular-dependent solutions in cylindrical dielectric

waveguides. This superposition is named as *HE* or *EH* according to whether the *TE* or *TM* term dominates in a suitable norm. The eigenvalue equations (2.28) corresponding to *HE* and *EH* modes are transformed as follow:

$$n_c^2 \eta_1^2 + (n_g^2 \eta_2 + \eta_2 n_c^2) \eta_1 + n_g^2 \eta_2^2 = (v n_{eff})^2 \left(\frac{V}{UW} \right)^4 \quad (2.33)$$

where $\eta_1 = J'_v(U)/UJ_v(U)$ and $\eta_2 = K'_v(W)/WK_v(W)$

Two group of roots will be obtain by solving this quadratic equation of η_1 ,

$$\eta_1 = \frac{-(n_g^2 \eta_2 + \eta_2 n_c^2) \pm \sqrt{(n_g^2 \eta_2 + \eta_2 n_c^2)^2 - 4n_c^2 \left[n_g^2 \eta_2^2 - (v n_{eff})^2 \left(\frac{V}{UW} \right)^4 \right]}}{2n_c^2} \quad (2.34)$$

Two equations derived from these two roots correspond to two families of hybrid modes, i.e. *HE* and *EH* mode. One of them, which gives dominant *HE*₁₁ mode, corresponds to the *HE* mode while the other one corresponds to the *EH* mode. Sign “+” is designated to represents *EH* mode while sing “-” represents *HE* mode.^{8 9}

2.3 Value Range of Effective Index

2.3.1 Value Range

The eigenvalue equations for HE and EH modes have solutions only within limited ranges of the parameter U and W . Furthermore, the effective indices n_{eff} , solutions to the eigenvalue equation, fall into limited value range, which is formed by two boundaries of the limit $W \rightarrow 0$, and $W \rightarrow \infty$. It is very helpful to know the value range of effective range as we investigate the modal characteristics of optical waveguides, for example, the single-mode condition.

2.3.2 Cutoff Condition

The value of effective index, at which β vanished, is called the cutoff condition. At the value below the cutoff condition, β becomes purely imaginary, the propagation factor $\exp(i\beta z)$ becomes an exponentially decaying function and the corresponding mode is said to β evanescent or non-propagating, or the mode is cutoff.

The wave function is the solution of the wave equation subject to boundary conditions. We know that the wave equations in the conventional fibre are combinations of first or second kind of Bessel functions. Thus, we could express wave functions with first and second kind of Bessel functions, while modal parameters V , U and W are factors of arguments of these Bessel function. $K_v(Wr/\rho)$ is used to express the outmost layer's wave function. As the increasing of W , the field expressed

with $K_\nu(Wr/\rho)$ is more tightly confined to the inside of the guide. As W decrease, the field penetrates more and more into the outer region. Finally, when $W \rightarrow 0$, the field detaches itself from the guide and begins to radiate away from it. Under this condition, $W \rightarrow 0$, by definition, the cutoff in dielectric waveguide occurs when the effective index n_{eff} becomes equal to the refractive index of the outer region n_g , and as a result, propagation along the axis of the structure can no longer be sustained. The modes below the cutoff condition are called radiation modes in contrast to the guided modes which exist above the cutoff condition.

Assuming $W \rightarrow 0$, the cutoff condition could be derived from the eigenvalue equation:⁷

Table 1 Cutoff Conditions of Two Layer Fibre

Mode	Cutoff Condition ($W \rightarrow 0$)
TE_{0m} and TM_{0m}	$J_0(U) = 0$
HE_{vm}	$\begin{cases} J_1(U) = 0 & (\text{with } U = 0) & \nu = 1 \\ \frac{UJ_{\nu-2}(U)}{(\nu-1)J_{\nu-1}(U)} = -\frac{2\Delta}{1-2\Delta} & \nu > 1 \end{cases}$ <p style="text-align: center;">where $\Delta = \frac{n_c^2 - n_g^2}{2n_c^2}$</p>
EH_{vm}	$J_\nu(U) = 0 \quad (U \neq 0)$

2.3.3 Far-from-cutoff Condition

As $W \rightarrow \infty$, from the definition of second kind of modified Bessel function, all the modal power is confined in the core. This is called far-from-cutoff condition. If $k\rho$ in the equation (2.13) tends to infinity, we will have $W \rightarrow \infty$, i.e. the far-from-cutoff condition. As the $n_{\text{eff}} \rightarrow n_{\text{core}}$, or $n_{\text{eff}} \rightarrow n_1$, U , which is the products of infinity $k\rho$ and zero $\sqrt{n_1^2 - n_{\text{eff}}^2}$, remains finite. The eigenvalue equation will develop to a function of modal parameter U at the limit of $W \rightarrow \infty$. It will give us the far-from-cutoff expressions to solve this equation. The effective index varies in the range formed by the cutoff and the far-from-cutoff conditions. Letting $W \rightarrow \infty$, we will have the far-from-cutoff conditions of the two layer dielectric waveguides as Table 2.⁷

Table 2 The Far-from-Cutoff Conditions of Two Layer Fibre

Mode	Far-from-cutoff Conditions ($W \rightarrow \infty$)
TE_{0m} and TM_{0m}	$J_1(U) = 0 \quad (U \neq 0)$
HE_{vm}	$J_{v-1}(U) = 0 \quad (U \neq 0)$
EH_{vm}	$J_{v+1}(U) = 0 \quad (U \neq 0)$

2.4 Conclusion

Except the axial symmetric transverse modes, TE_{0m} and TM_{0m} modes, all the modes are hybrid modes, HE_{vm} or EH_{vm} .

From Table 1, we find that the “ U ” in the cutoff equation has discrete roots. For example, the cutoff values of mode TE_{0m} are the roots of the equation $J_0(U) = 0$, i.e. the value of corresponding $U_c = 2.41, 5.52, 8.65, 11.79$, etc... (zeros of J_0). Whereas the far-from-cutoff values of mode TE_{0m} are the roots of the equation of $J_1(U) = 0$, i.e. the value of corresponding $U_\infty = 3.83, 7.02, 10.17, 13.32$, etc... (zeros of $J_1, U \neq 0$). The eigenvalue of modes TE_{0m}, U_{0m} has a single root between the two boundaries, U_c and U_∞ . Then for the first three values of U_{0m} , we have:

$$\begin{aligned} 2.41 &\leq U_{01} \leq 3.83 \\ 5.52 &\leq U_{02} \leq 7.02 \\ 8.65 &\leq U_{03} \leq 10.17 \end{aligned} \tag{2.35}$$

For the modes $EH_{\nu m}$, the ν is given, the values of corresponding U_c are the roots of the equation $J_\nu(U) = 0$ ($U \neq 0$), the first root of “ U ” corresponds to the cutoff condition of first mode, and the m^{th} root of “ U ” corresponds to the cutoff condition of mode $EH_{\nu m}$, and so on. The values of corresponding U_∞ are the roots of the equation $J_{\nu+1}(U) = 0$ ($U \neq 0$). The first root of “ U ” corresponds to the cutoff condition of first mode, and the m^{th} root of “ U ” corresponds to the far-from-cutoff condition of mode $EH_{\nu m}$, and so on. The eigenvalue of each EH mode for a given ν has a single root between the intervals formed by U_c and U_∞ . (m^{th} zero of $J_\nu \leq U_{\nu m} \leq m^{\text{th}}$ zero of $J_{\nu+1}$, where $U \neq 0$ is not included)

Although the situation of HE_{vm} is more complicated, we can still reach the same conclusion. The eigenvalue U_{vm} varies in the range formed by the U_c (cutoff), and U_∞ (far-from-cutoff).

The mode HE_{11} is the single mode with zero cutoff value, which always exists in the fibre with step-index profile.

$$0 \leq U_{11} \leq 2.41 \quad (2.36)$$

From the definition of modal parameters, we have

$$n_{eff} = n_c \sqrt{1 - 2\Delta(U/V)^2} \quad (2.37)$$

where $2\Delta = 1 - n_g^2/n_c^2$.

For each of the roots of the cutoff or the far-from-cutoff equations, the U_c (cutoff), or U_∞ (far-from-cutoff) has its corresponding effective index, named n_{eff} (cutoff) or n_{eff} (far-from-cutoff).

If we plot the n_{eff} (cutoff) or n_{eff} (far-from-cutoff) with the effective index together, we will find that the effective index is in the region formed by the n_{eff} (cutoff) or n_{eff} (far-from-cutoff).

From Table 1 and Table 2, it can be easily proved analytically that the effective indices of modes HE_{vm} and EH_{vm} are in the sequence for a given order v , and that there is no overlapping of modes for a given order v in the two layer structures.

As the modes in optical fibre are investigated, a primary assumption is that the cladding radius extends to infinity, or the ratio of cladding radius to the core radius is big enough. Then the optical fibre is regarded as an ordinary two layer dielectric waveguide, and the eigenvalue equation, the cutoff and the far-from-cutoff expressions of TE , TM , and even HE and EH modes can be easily obtained. But if this assumption can not be satisfied, the conventional two layer optical fibre becomes a three layer or multilayer dielectric structure, and consequently the investigation of modal characteristics and mode classification will be more complicated.

CHAPTER 3

CLASSIFICATION OF MODES IN THREE LAYER FIBRES

3.1 Introduction

With the rapid advancement of optical fibre communications, a variety of optical fibre component designs have been proposed and employed in various applications due to their specific modal characteristics, e.g. the three layer optical fibre or multilayer optical fibre is used to design the dispersion-shifted and dispersion-flattened fibre.¹⁶ As we discuss the conventional optical fibre above, a primary assumption is that the cladding radius extends to infinity, or the ratio of cladding radius to the core radius is big enough. Then the optical fibre is regarded as a two layer dielectric optical waveguide, and the eigenvalue equation, the cutoff and the far-from-cutoff conditions of symmetric modes TE_{0m} , TM_{0m} and non-symmetric modes HE_{vm} , EH_{vm} , can be easily obtained.

But if the ratio is not big enough, the structure of optical fibre with step-index profile will become a three layer dielectric waveguide, or a three layer cladded fibre structure.

To deal with the three layer structure step-profile dielectric waveguide, the eigenvalue equation method of *Snyder* is still regarded as a proper method. *A. Safaai-Jazi et al*,^{8 9} *Achint Kapoor et al*¹⁴ proposed the methods of eigenvalue equation of modes to classify the hybrid modes in various index profile of three layer cylindrical dielectric waveguides, like the dielectric rod or the dielectric tube. Comparing their methods, *Achint Kapoor et al*¹⁴ chose the modal term $\eta_4 = -K'_v(W)/WK_v(W)$ in their quadratic eigenvalue equation, which could not be employed to obtain the cutoff and the far-from-cutoff values. On the other hand, the eigenvalue equation of *A. Safaai-Jazi et al*^{8 9} is a quadratic equation of modal term $\eta_1 = -J'_v(x)/xJ_v(x)$, where, $x = \alpha_1 a$ is the modal parameter of the core of the waveguide. The two sets of roots of this quadratic equation could be used to designate the hybrid modes, *HE* and *EH* modes in arbitrary three layer structures. The method of *A. Safaai-Jazi et al*^{8 9} is appropriate as a global scheme used to designate hybrid modes in all the structures of cylindrical dielectric waveguides.

Out of the various important aspects of dielectric waveguides, the cutoff conditions play a major role in the design of such structures and the selection of operation wavelength. The above-mentioned articles give the cutoff values of two and three layer dielectric waveguides. Hardly mentioned are the far from cutoff values of modal parameters. We believe

that it is of the same importance with the cutoff condition. Because the two values form a range, in which the mode effective index varies, it will help us to characterize the modes of dielectric waveguides more precisely and efficiently.

Comparing the two layer structure, the derivation of the cutoff and the far-from-cutoff expressions should be very complicated. In this paper, the global scheme of *Safaai-Jazi and Yip*^{8 9} is employed to conduct our mode designation and analysis. The final purpose is to specify the effective index range bounded by the cutoff and the far-from-cutoff conditions with the aid of the eigenvalue equation method.

Because the transverse components of the fields can be expressed in terms of the axial components, the vector wave equation becomes two identical partial differential equations of longitudinal components E_z and H_z . The eigenvalue equation can be obtained through the continuity conditions of longitudinal and tangential components at one interface. By setting the effective indices of modes tend to the indices of two adjacent media, the cutoff and far-from-cutoff occur, thus giving the cutoff and the far-from-cutoff expressions of modal parameters. This is the eigenvalue (characteristic) equation method used widely in two layer cylindrical waveguides.

Similarly, in three layer structures, the effective index of guided modes could be investigated by determining the two boundaries of the range of modal parameters using the eigenvalue equation method. Because there are two different boundaries in three layer structures, the tangential and longitudinal components of the fields have to be continuous at these two boundaries. An 8×8 matrix will be obtained by letting axial and tangential component to comply the boundary conditions. The determinant of the 8×8 matrix must vanish in order to have non-trivial solutions of the coefficients.

Thus a quadratic equation of the propagation constant is obtained. This quadratic equation has two groups of roots, called eigenvalue equation (characteristic equation), corresponding to the modes HE and EH .

3.2 Eigenvalue Equation

3.2.1 Introduction

Depending on the index profile of the three layer structures, it can be classified into cladded fibre, tubular and W -type structure. Step-index three layer structures have 5 useful combinations of profile of index; it is extremely difficult to find an appropriate analytic characteristic equation

to define all the three layer dielectric waveguides. Compared with the two layer structures, the derivation of the eigenvalue equation and the cutoff, the far-from-cutoff expressions is very complicated. Until now, only *Safaai-Jazi and Yip's*^{8 9} global analytic expressions of eigenvalue equation are applicable to some most popular three layer structures, as cladded fibre, tubular and W-type structure. *Achint Kapoor and G.S. Singh*¹⁴ made a small modification to *Safaai-Jazi and Yip's*^{8 9} method.

3.2.2 Index Profile

a) Cladded Fibre

The index profile of cladded fibre satisfies the condition

$$n_1 > n_2 > n_3$$

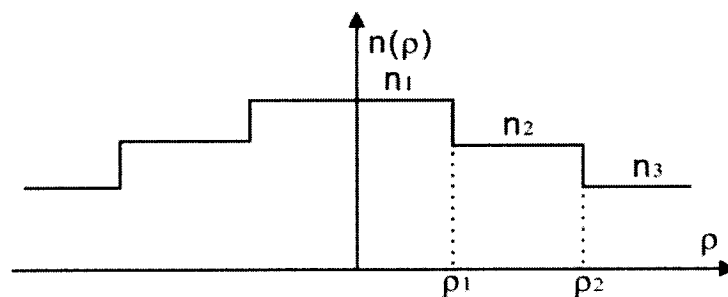


Fig. 3 Index profile of cladded fibre

b) Dielectric Tube Fibre

The index profile of tubular fibre satisfies three conditions

$$n_2 > n_1 = n_3$$

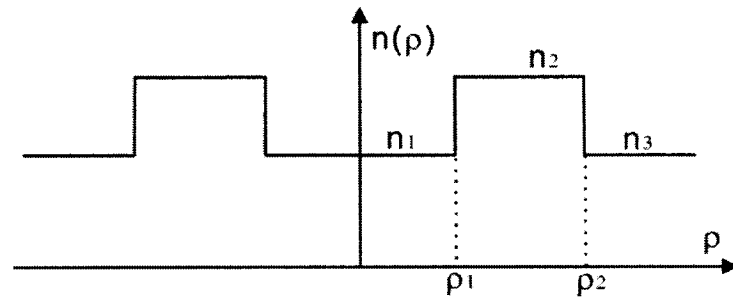


Fig. 4 Index profile of tube fibre I

$$n_2 > n_1 > n_3$$

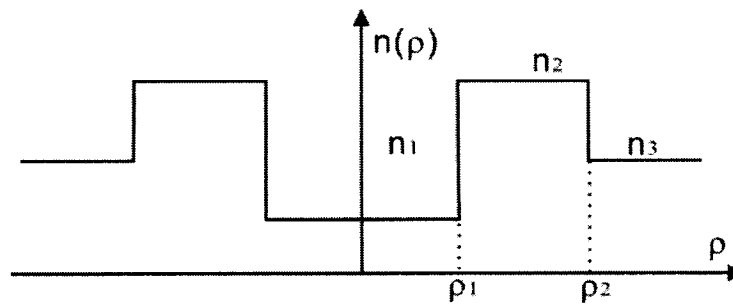


Fig. 5 Index profile of tube fibre II

$$n_2 > n_3 > n_1$$

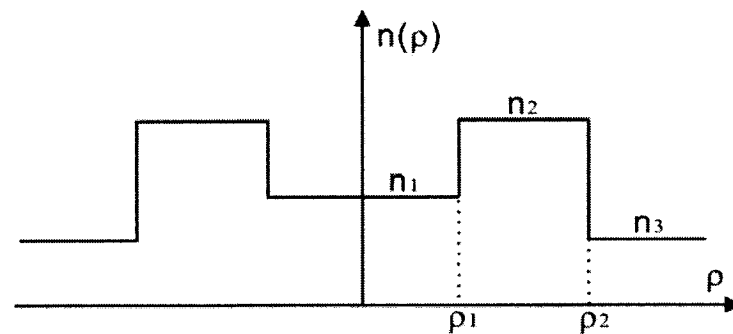


Fig. 6 Index profile of tube fibre III

c) *W*-type Fibre

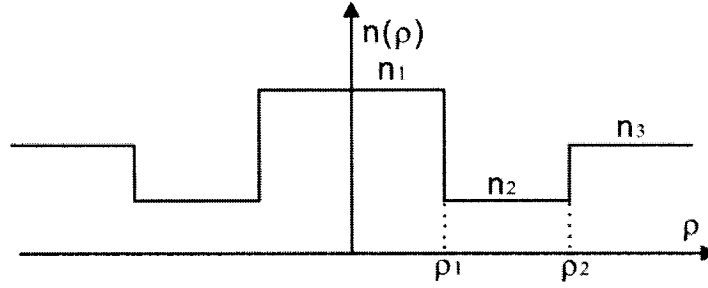


Fig. 7 Index profile of W-type fibre

3.2.3 The Maxwell Equation and Wave Equation

The three layer structures discussed here is assumed to be a non-absorbing, ideal dielectric structure, source free, perfect circular on the cross section and uniform along its axis. The time and z -dependence of fields expressed as $\exp[i(\beta z - \omega t)]$ is common to all field components, where β is the axial propagation constant.

Because of the concentric, symmetric section of the three layer structure, the method of separation of variables is still applicable. The field can be expressed as

$$\Psi(r, \phi, z, t) = R(r)\Phi(\phi)e^{i(\beta z - \omega t)} \quad (3.1)$$

where $\Psi(r, \phi, z, t)$ represents longitudinal component of electric or magnetic field and expression (3.1) is only applicable to the circular symmetric waveguide. $\Phi(\phi)$ is expressed as :

$$\Phi(\phi) = \begin{cases} f_v(\phi) \\ g_v(\phi) \end{cases} \quad (3.2)$$

$$\begin{aligned} f_\nu(\phi) &= \begin{cases} \cos(\nu\phi) \\ \sin(\nu\phi) \end{cases} \\ g_\nu(\phi) &= \begin{cases} -\sin(\nu\phi) \\ \cos(\nu\phi) \end{cases} \end{aligned} \quad (3.3)$$

where ν denotes the azimuthal number.

In the three layer step index structure, the variation of the index is zero, except in the two interfaces. Hence, the term in the vector wave equations (3.18) $dLnn^2/dr$ is equal to zero. The wave equation is simplified as:

$$\frac{d^2 R(r)}{dr^2} + \frac{1}{r} \frac{dR(r)}{dr} + \left[k_0^2 (\epsilon_r - n_{eff}^2) - \frac{\nu^2}{r^2} \right] R(r) = 0 \quad (3.4)$$

3.2.4 Boundary Conditions

A three layer structure is divided into three regions, region *I*, $0 < r < \rho$, region *II*, $\rho_1 < r < \rho_2$ and region *III*, $\rho_2 < r < \infty$. The outermost layer, region *III*, extends to infinity. The fields in each region are solutions to the above wave equation (3.4) subject to boundary conditions as follows:

$$\begin{aligned} e_z(\rho_1 - 0) &= e_z(\rho_1 + 0) & h_z(\rho_1 - 0) &= h_z(\rho_1 + 0) \\ e_\phi(\rho_1 - 0) &= e_\phi(\rho_1 + 0) & h_\phi(\rho_1 - 0) &= h_\phi(\rho_1 + 0) \\ e_z(\rho_2 - 0) &= e_z(\rho_2 + 0) & h_z(\rho_2 - 0) &= h_z(\rho_2 + 0) \\ e_\phi(\rho_2 - 0) &= e_\phi(\rho_2 + 0) & h_\phi(\rho_2 - 0) &= h_\phi(\rho_2 + 0) \end{aligned} \quad (3.5)$$

3.2.5 Eigenvalue Equation of Hybrid mode *HE* and *EH*

In the j^{th} layer, the wave equation is rewritten as:

$$\frac{d^2 R(r)}{dr^2} + \frac{1}{r} \frac{dR(r)}{dr} + \left[k_0^2 (n_j^2 - n_{\text{eff}}^2) - \frac{\nu^2}{r^2} \right] R(r) = 0 \quad (3.6)$$

where $j = 1, 2, 3$

If $n_j > n_{\text{eff}}$, the above equation is the first kind of Bessel differential equation, its solution is the sum of the first kind of Bessel function and the modified first kind of Bessel functions

$$R(r) = a_{\nu j} J_{\nu}(\alpha_j r) + b_{\nu j} Y_{\nu}(\alpha_j r) \quad (3.7)$$

where $\alpha_j = k_0 |n_j^2 - n_{\text{eff}}^2|^{1/2}$

If $n_j < n_{\text{eff}}$, the wave equation becomes the second kind of Bessel differential equation, its solution is the sum of the second kind of Bessel functions

$$R(r) = a_{\nu j} I_{\nu}(\alpha_j r) + b_{\nu j} K_{\nu}(\alpha_j r) \quad (3.8)$$

Due to the function $Y_{\nu}(x)$ and $I_{\nu}(x)$ tending to infinity as the argument x tends to zero or infinity, the two functions should be dropped off in the innermost and outermost layer's field. Thus, the field expression depends on the sign of $n_j - n_{\text{eff}}$. A function $Z_{\nu k}$ can be used to define the longitudinal field components in three layer structures, “ ν ” is azimuthal number and $k = 1, 2, 3, 4$.

Thus, a generalized expression for the field of three layer structure is written as:

$$\Psi(r, \phi, z, t) = \Phi(\phi) e^{i(\beta z - \omega t)} \begin{cases} a_{vj} Z_{v,1}(\alpha_1 r) & 0 \leq r \leq \rho_1 \\ b_{vj} Z_{v,2}(\alpha_2 r) + c_{vj} Z_{v,3}(\alpha_2 r) & 0 \leq r \leq \rho_2 \\ d_{vj} Z_{v,4}(\alpha_3 r) & r > \rho_2 \end{cases} \quad (3.9)$$

To include all the three primary fibre structures, cladded, tubular and *W*-type, into this generalized expression, where an “*s*” is used to evaluate which kind of Bessel functions will be employed to express the longitudinal field components.

$$\begin{cases} s_j = 1 & n_j > n_{eff} \\ s_j = -1 & n_j < n_{eff} \end{cases} \quad (3.10)$$

$j = 1, 2, 3$

subscript j represents the j^{th} layer of the three layer structure.

The function Z_{vk} is defined in Table 3.

For given j and known effective index, the sign of $n_j - n_{eff}$ could be used to determine the exact the field expression of the j^{th} layer.

Table 3 The generalized function

$Z_{v,1}$		$Z_{v,2}$		$Z_{v,3}$		$Z_{v,4}$
$s_1 = 1$	$s_1 = -1$	$s_2 = 1$	$s_2 = -1$	$s_2 = 1$	$s_2 = -1$	$s_3 = -1$
$J_v(x)$	$I_v(x)$	$J_v(x)$	$I_v(x)$	$Y_v(x)$	$K_v(x)$	$K_v(x)$

The longitudinal components of electric and magnetic fields are

expressed as follows:

$$e_z(r, \phi) = f_v(\phi) \begin{cases} a_1 \frac{Z_{v,1}\left(x \frac{r}{\rho_1}\right)}{Z_{v,1}(x)} & 0 \leq r \leq \rho_1 \\ a_2 \frac{Z_{v,2}\left(U_1 \frac{r}{\rho_1}\right)}{Z_{v,2}(U_1)} + a_3 \frac{Z_{v,3}\left(U_1 \frac{r}{\rho_1}\right)}{Z_{v,3}(U_1)} & \rho_1 \leq r \leq \rho_2 \\ a_4 \frac{Z_{v,4}\left(W \frac{r}{\rho_2}\right)}{Z_{v,4}(W)} & r > \rho_2 \end{cases} \quad (3.11)$$

and

$$h_z(r, \phi) = g_v(\phi) \begin{cases} a_5 \frac{Z_{v,1}\left(x \frac{r}{\rho_1}\right)}{Z_{v,1}(x)} & 0 \leq r \leq \rho_1 \\ a_6 \frac{Z_{v,2}\left(U_1 \frac{r}{\rho_1}\right)}{Z_{v,2}(U_1)} + a_7 \frac{Z_{v,3}\left(U_1 \frac{r}{\rho_1}\right)}{Z_{v,3}(U_1)} & \rho_1 \leq r \leq \rho_2 \\ a_8 \frac{Z_{v,4}\left(W \frac{r}{\rho_2}\right)}{Z_{v,4}(W)} & r > \rho_2 \end{cases} \quad (3.12)$$

where

$$x = \alpha_1 \rho_1, \quad U_1 = \alpha_2 \rho_1, \quad U_2 = \alpha_2 \rho_2, \quad W = \alpha_3 \rho_2 \quad (3.13)$$

$$f_v(\phi) = \begin{cases} \cos(v\phi) \\ \sin(v\phi) \end{cases} \quad g_v(\phi) = \begin{cases} -\sin(v\phi) \\ \cos(v\phi) \end{cases} \quad (3.14)$$

Similarly, as in the two layer structure processing, we obtain all

the components in three layer structures as follows:

In the core: $0 \leq r \leq \rho_1$

$$e_z = \frac{Z_{v,1}\left(x \frac{r}{\rho_1}\right)}{Z_{v,1}(x)} f_v(\phi) a_{v1} \quad (3.15)$$

$$e_r = s_1 \frac{i\rho_1^2}{x^2} f_v(\phi) \left\{ \frac{Z'_{v,1}\left(x \frac{r}{\rho_1}\right)}{Z_{v,1}(x)} \beta \frac{x}{\rho_1} a_{v1} - \frac{Z_{v,1}\left(x \frac{r}{\rho_1}\right)}{Z_{v,1}(x)} \sqrt{\frac{\mu_0}{\epsilon_0}} \frac{k}{r} \nu a_{v5} \right\} \quad (3.16)$$

$$e_\phi = s_1 \frac{i\rho_1^2}{x^2} g_v(\phi) \left\{ \frac{Z_{v,1}\left(x \frac{r}{\rho_1}\right)}{Z_{v,1}(x)} \nu \frac{\beta}{r} a_{v1} - \frac{Z'_{v,1}\left(x \frac{r}{\rho_1}\right)}{Z_{v,1}(x)} \sqrt{\frac{\mu_0}{\epsilon_0}} k \frac{x}{\rho_1} a_{v5} \right\} \quad (3.17)$$

$$h_z = \frac{Z_{v,1}\left(x \frac{r}{\rho_1}\right)}{Z_{v,1}(x)} g_v(\phi) a_{v5} \quad (3.18)$$

$$h_r = s_1 \frac{i\rho_1^2}{x^2} g_v(\phi) \left\{ \frac{Z'_{v,1}\left(x \frac{r}{\rho_1}\right)}{Z_{v,1}(x)} \beta \alpha_1 \frac{x}{\rho_1} a_{v5} - \frac{Z_{v,1}\left(x \frac{r}{\rho_1}\right)}{Z_{v,1}(x)} \sqrt{\frac{\epsilon_0}{\mu_0}} \frac{kn_1^2}{r} \nu a_{v1} \right\} \quad (3.19)$$

$$h_\phi = s_1 \frac{i\rho_1^2}{x^2} f_v(\phi) \left\{ -\frac{Z_{v,1}\left(x \frac{r}{\rho_1}\right)}{Z_{v,1}(x)} \nu \frac{\beta}{r} a_{v5} + \frac{Z'_{v,1}\left(x \frac{r}{\rho_1}\right)}{Z_{v,1}(x)} \sqrt{\frac{\epsilon_0}{\mu_0}} kn_1^2 \frac{x}{\rho_1} a_{v1} \right\} \quad (3.20)$$

In the first cladding: $\rho_1 \leq r \leq \rho_2$

$$e_z = \left[\frac{Z_{v,2} \left(U_1 \frac{r}{\rho_1} \right)}{Z_{v,2}(U_1)} a_{v2} + \frac{Z_{v,3} \left(U_1 \frac{r}{\rho_1} \right)}{Z_{v,3}(U_1)} a_{v3} \right] f_v(\phi)$$

or

$$(3.21)$$

$$= \left[\frac{Z_{v,2} \left(U_2 \frac{r}{\rho_2} \right)}{Z_{v,2}(U_2)} a_{v2} + \frac{Z_{v,3} \left(U_2 \frac{r}{\rho_2} \right)}{Z_{v,3}(U_2)} a_{v3} \right] f_v(\phi)$$

$$e_r = s_2 \frac{i\rho_1^2}{U_1^2} f_v(\phi) \left\{ \frac{U_1}{\rho_1} \beta \left[\frac{Z'_{v,2} \left(U_1 \frac{r}{\rho_1} \right)}{Z_{v,2}(U_1)} a_{v2} + \frac{Z'_{v,3} \left(U_1 \frac{r}{\rho_1} \right)}{Z_{v,3}(U_1)} a_{v3} \right] \right. \\ \left. - \sqrt{\frac{\mu_0}{\epsilon_0}} \frac{k}{r} v \left[\frac{Z_{v,2} \left(U_1 \frac{r}{\rho_1} \right)}{Z_{v,2}(U_1)} a_{v6} + \frac{Z_{v,3} \left(U_1 \frac{r}{\rho_1} \right)}{Z_{v,3}(U_1)} a_{v7} \right] \right\}$$

or

$$= s_2 \frac{i\rho_2^2}{U_2^2} f_v(\phi) \left\{ \frac{U_2}{\rho_2} \beta \left[\frac{Z'_{v,2} \left(U_2 \frac{r}{\rho_2} \right)}{Z_{v,2}(U_2)} a_{v2} + \frac{Z'_{v,3} \left(U_2 \frac{r}{\rho_2} \right)}{Z_{v,3}(U_2)} a_{v3} \right] \right. \\ \left. - \sqrt{\frac{\mu_0}{\epsilon_0}} \frac{k}{r} v \left[\frac{Z_{v,2} \left(U_2 \frac{r}{\rho_2} \right)}{Z_{v,2}(U_2)} a_{v6} + \frac{Z_{v,3} \left(U_2 \frac{r}{\rho_2} \right)}{Z_{v,3}(U_2)} a_{v7} \right] \right\} \quad (3.22)$$

$$h_z = \left[\frac{Z_{v,2} \left(U_1 \frac{r}{\rho_1} \right)}{Z_{v,3}(U_1)} a_{v6} + \frac{Z_{v,3} \left(U_1 \frac{r}{\rho_1} \right)}{Z_{v,3}(U_1)} a_{v7} \right] g_v(\phi)$$

or

$$= \left[\frac{Z_{v,2} \left(U_2 \frac{r}{\rho_2} \right)}{Z_{v,3}(U_2)} a_{v6} + \frac{Z_{v,3} \left(U_2 \frac{r}{\rho_2} \right)}{Z_{v,3}(U_2)} a_{v7} \right] g_v(\phi) \quad (3.23)$$

$$h_r = s_2 \frac{i\rho_1^2}{U_1^2} g_v(\phi) \left\{ \beta \frac{U_1}{\rho_1} \left[\frac{Z'_{v,2} \left(U_1 \frac{r}{\rho_1} \right)}{Z_{v,3}(U_1)} a_{v6} + \frac{Z'_{v,3} \left(U_1 \frac{r}{\rho_1} \right)}{Z_{v,3}(U_1)} a_{v7} \right] \right.$$

$$\left. - \sqrt{\frac{\varepsilon_0}{\mu_0}} \frac{kn_2^2}{r} v \left[\frac{Z_{v,2} \left(U_1 \frac{r}{\rho_1} \right)}{Z_{v,2}(U_1)} a_{v2} + \frac{Z_{v,3} \left(U_1 \frac{r}{\rho_1} \right)}{Z_{v,3}(U_1)} a_{v3} \right] \right\}$$

or

$$= s_2 \frac{i\rho_2^2}{U_2^2} g_v(\phi) \left\{ \beta \frac{U_2}{\rho_2} \left[\frac{Z'_{v,2} \left(U_2 \frac{r}{\rho_2} \right)}{Z_{v,3}(U_2)} a_{v6} + \frac{Z'_{v,3} \left(U_2 \frac{r}{\rho_2} \right)}{Z_{v,3}(U_2)} a_{v7} \right] \right.$$

$$\left. - \sqrt{\frac{\varepsilon_0}{\mu_0}} \frac{kn_2^2}{r} v \left[\frac{Z_{v,2} \left(U_2 \frac{r}{\rho_2} \right)}{Z_{v,2}(U_2)} a_{v2} + \frac{Z_{v,3} \left(U_2 \frac{r}{\rho_2} \right)}{Z_{v,3}(U_2)} a_{v3} \right] \right\} \quad (3.24)$$

$$\begin{aligned}
h_\phi &= s_2 \frac{i\rho_1^2}{U_1^2} f_v(\phi) \left\{ -\frac{\beta}{r} v \left[\frac{Z_{v,2}\left(U_1 \frac{r}{\rho_1}\right)}{Z_{v,2}(U_1)} a_{v6} + \frac{Z_{v,3}\left(U_1 \frac{r}{\rho_1}\right)}{Z_{v,3}(U_1)} a_{v7} \right] \right. \\
&\quad \left. + \sqrt{\frac{\varepsilon_0}{\mu_0}} k n_2^2 \frac{U_1}{\rho_1} \left[\frac{Z'_{v,2}\left(U_1 \frac{r}{\rho_1}\right)}{Z_{v,2}(U_1)} a_{v2} + \frac{Z'_{v,3}\left(U_1 \frac{r}{\rho_1}\right)}{Z_{v,3}(U_1)} a_{v3} \right] \right\} \\
&\text{or} \\
&= s_2 \frac{i\rho_2^2}{U_2^2} f_v(\phi) \left\{ -\frac{\beta}{r} v \left[\frac{Z_{v,2}\left(U_2 \frac{r}{\rho_2}\right)}{Z_{v,2}(U_2)} a_{v6} + \frac{Z_{v,3}\left(U_2 \frac{r}{\rho_2}\right)}{Z_{v,3}(U_2)} a_{v7} \right] \right. \\
&\quad \left. + \sqrt{\frac{\varepsilon_0}{\mu_0}} k n_2^2 \frac{U_2}{\rho_2} \left[\frac{Z'_{v,2}\left(U_2 \frac{r}{\rho_2}\right)}{Z_{v,2}(U_2)} a_{v2} + \frac{Z'_{v,3}\left(U_2 \frac{r}{\rho_2}\right)}{Z_{v,3}(U_2)} a_{v3} \right] \right\} \quad (3.25)
\end{aligned}$$

In the second cladding: $\rho_2 \leq r \leq \infty$

$$e_z = \frac{Z_{v,4}\left(W \frac{r}{\rho_2}\right)}{Z_{v,4}(W)} f_v(\phi) a_{v4} \quad (3.26)$$

$$e_r = s_3 \frac{i\rho_2^2}{W^2} f_v(\phi) \left\{ \frac{Z'_{v,4}\left(W \frac{r}{\rho_2}\right)}{Z_{v,4}(W)} \beta a_{v4} - \sqrt{\frac{\mu_0}{\varepsilon_0}} \frac{k}{r} v \frac{Z_{v,4}\left(W \frac{r}{\rho_2}\right)}{Z_{v,4}(W)} a_{v8} \right\} \quad (3.27)$$

$$e_\phi = s_3 \frac{i\rho_2^2}{W^2} g_v(\phi) \left\{ \frac{Z_{v,4}\left(W \frac{r}{\rho_2}\right)}{Z_{v,4}(W)} \frac{\beta}{r} v a_{v4} - \frac{Z'_{v,4}\left(W \frac{r}{\rho_2}\right)}{Z_{v,4}(W)} \sqrt{\frac{\mu_0}{\varepsilon_0}} k \frac{W}{\rho_2} a_{v8} \right\} \quad (3.28)$$

$$e_r = s_3 \frac{i\rho_2^2}{W^2} f_v(\phi) \left\{ \frac{Z'_{v,4} \left(W \frac{r}{\rho_2} \right)}{Z_{v,4}(W)} \beta a_{v,4} - \frac{Z_{v,4} \left(W \frac{r}{\rho_2} \right)}{Z_{v,4}(W)} \sqrt{\frac{\mu_0}{\varepsilon_0}} \frac{k}{r} v a_{v,8} \right\} \quad (3.29)$$

$$e_\phi = s_3 \frac{i\rho_2^2}{W^2} g_v(\phi) \left\{ \frac{Z_{v,4} \left(W \frac{r}{\rho_2} \right)}{Z_{v,4}(W)} \beta v a_{v,4} - \frac{Z'_{v,4} \left(W \frac{r}{\rho_2} \right)}{Z_{v,4}(W)} \sqrt{\frac{\mu_0}{\varepsilon_0}} k \frac{W}{\rho_2} a_{v,8} \right\} \quad (3.30)$$

$$h_z = \frac{Z_{v,4} \left(W \frac{r}{\rho_2} \right)}{Z_{v,4}(W)} g_v(\phi) a_{v,8} \quad (3.31)$$

$$h_r = s_3 \frac{i\rho_2^2}{W^2} g_v(\phi) \left\{ \frac{Z'_{v,4} \left(W \frac{r}{\rho_2} \right)}{Z_{v,4}(W)} \beta \frac{W}{\rho_2} a_{v,8} - \frac{Z_{v,4} \left(W \frac{r}{\rho_2} \right)}{Z_{v,4}(W)} \sqrt{\frac{\varepsilon_0}{\mu_0}} \frac{k n_3^2}{r} v a_{v,4} \right\} \quad (3.32)$$

$$h_\phi = s_3 \frac{i\rho_2^2}{W^2} f_v(\phi) \left\{ -\frac{Z_{v,4} \left(W \frac{r}{\rho_2} \right)}{Z_{v,4}(W)} \beta v a_{v,8} + \frac{Z'_{v,4} \left(W \frac{r}{\rho_2} \right)}{Z_{v,4}(W)} \sqrt{\frac{\varepsilon_0}{\mu_0}} k n_3^2 \frac{W}{\rho_2} a_{v,4} \right\} \quad (3.33)$$

Introducing $\eta_1, \eta_2, \eta_3, \eta_4, \eta_5, \eta_6$ which are defined as follow:

$$\eta_1 = \frac{s_1}{x} \frac{Z'_{v,1}(x)}{Z_{v,1}(x)} \quad (3.34)$$

$$\eta_2 = \frac{s_2}{U_1} \frac{Z'_{v,2}(U_1)}{Z_{v,2}(U_1)} \quad (3.35)$$

$$\eta_3 = \frac{s_2}{U_1} \frac{Z'_{v,3}(U_1)}{Z_{v,3}(U_1)} \quad (3.36)$$

$$\eta_4 = \frac{s_2}{U_2} \frac{Z'_{v,2}(U_2)}{Z_{v,2}(U_2)} \quad (3.37)$$

$$\eta_5 = \frac{s_2}{U_2} \frac{Z'_{v,1}(U_2)}{Z_{v,3}(U_2)} \quad (3.38)$$

$$\eta_6 = \frac{s_3}{W} \frac{K'_v(W)}{K_v(W)} \quad (3.39)$$

Applying the boundary conditions of longitudinal components continuity at $r = \rho_1$ and $r = \rho_2$ of electric and magnetic field, we have:

$$e_z(\rho_1 - 0) = e_z(\rho_1 + 0) \quad (3.40)$$

$$e_z(\rho_2 - 0) = e_z(\rho_2 + 0) \quad (3.41)$$

$$h_z(\rho_1 - 0) = h_z(\rho_1 + 0) \quad (3.42)$$

$$h_z(\rho_2 - 0) = h_z(\rho_2 + 0) \quad (3.43)$$

Four equations will be obtained as follow:

$$a_{v1} = a_{v2} + a_{v3} \quad (3.44)$$

$$a_{v2} + a_{v3} = a_{v4} \quad (3.45)$$

$$a_{v5} = a_{v6} + a_{v7} \quad (3.46)$$

$$a_{v6} + a_{v7} = a_{v8} \quad (3.47)$$

Applying the boundary conditions of angular components continuity at $r = \rho_1$ and $r = \rho_2$ of electric and magnetic field, we have:

$$e_{\phi}(\rho_1 - 0) = e_{\phi}(\rho_1 + 0) \quad (3.48)$$

$$e_{\phi}(\rho_2 - 0) = e_{\phi}(\rho_2 + 0) \quad (3.49)$$

$$h_{\phi}(\rho_1 - 0) = h_{\phi}(\rho_1 + 0) \quad (3.50)$$

$$h_{\phi}(\rho_2 - 0) = h_{\phi}(\rho_2 + 0) \quad (3.51)$$

Another four equations will be obtained as follow:

$$\begin{aligned} s_1 \frac{1}{x^2} \left\{ v \frac{\beta}{\rho_1} a_{v1} - \sqrt{\frac{\mu_0}{\varepsilon_0}} k \frac{x^2}{\rho_1} \eta_1 a_{v5} \right\} \\ = s_2 \frac{1}{U_1^2} \left\{ \frac{\beta}{\rho_1} v [a_{v2} + a_{v3}] - \sqrt{\frac{\mu_0}{\varepsilon_0}} k \frac{U_1^2}{\rho_1} [a_{v6} \eta_2 + a_{v7} \eta_3] \right\} \end{aligned} \quad (3.52)$$

$$\begin{aligned} s_2 \frac{1}{U_2^2} \left\{ \frac{\beta}{\rho_2} v [a_{v2} + a_{v3}] - \sqrt{\frac{\mu_0}{\varepsilon_0}} k \frac{U_2^2}{\rho_2} [a_{v6} \eta_4 + a_{v7} \eta_5] \right\} \\ = s_3 \frac{1}{W^2} \left\{ \frac{\beta}{\rho_2} v a_{v4} - \sqrt{\frac{\mu_0}{\varepsilon_0}} k \frac{W^2}{\rho_2} a_{v8} \eta_6 \right\} \end{aligned} \quad (3.53)$$

$$\begin{aligned} s_1 \frac{1}{x^2} \left\{ \sqrt{\frac{\varepsilon_0}{\mu_0}} k n_1^2 \frac{x}{\rho_1} \eta_1 a_{v1} - v \frac{\beta}{\rho_1} a_{v5} \right\} \\ = s_2 \frac{1}{U_1^2} \left\{ \sqrt{\frac{\varepsilon_0}{\mu_0}} k n_2^2 \frac{U_1^2}{\rho_1} [a_{v2} \eta_2 + a_{v3} \eta_3] - \frac{\beta}{\rho_1} v [a_{v6} + a_{v7}] \right\} \end{aligned} \quad (3.54)$$

$$\begin{aligned} s_2 \frac{1}{U_2^2} \left\{ \sqrt{\frac{\varepsilon_0}{\mu_0}} k n_2^2 \frac{U_2^2}{\rho_2} [a_{v2} \eta_4 + a_{v3} \eta_5] - \frac{\beta}{\rho_2} v [a_{v6} + a_{v7}] \right\} \\ = s_3 \frac{1}{W^2} \left\{ \sqrt{\frac{\varepsilon_0}{\mu_0}} k n_3^2 \frac{W^2}{\rho_2} a_{v4} \eta_6 - v \frac{\beta}{\rho_2} a_{v8} \right\} \end{aligned} \quad (3.55)$$

Rearranging these eight equations, eight linear equations of coefficient $a_1, a_2, a_3, a_4, a_5, a_6, a_7, a_8$ will be obtained as follow:

$$a_{v1} - a_{v2} - a_{v3} = 0 \quad (3.56)$$

$$a_{v2} + a_{v3} - a_{v4} = 0 \quad (3.57)$$

$$a_{v5} - a_{v6} - a_{v7} = 0 \quad (3.58)$$

$$a_{v6} + a_{v7} - a_{v8} = 0 \quad (3.59)$$

$$\begin{aligned} & \nu \frac{\beta}{\rho_1} a_{v1} - s_1 s_2 \frac{x^2}{U_1^2} \frac{\beta}{\rho_1} \nu a_{v2} - s_1 s_2 \frac{x^2}{U_1^2} \frac{\beta}{\rho_1} \nu a_{v3} - \sqrt{\frac{\mu_0}{\varepsilon_0}} k \frac{x^2}{\rho_1} \eta_1 a_{v5} \\ & + s_1 s_2 \sqrt{\frac{\mu_0}{\varepsilon_0}} k \frac{x^2}{\rho_1} \eta_2 a_{v6} + s_1 s_2 \sqrt{\frac{\mu_0}{\varepsilon_0}} k \frac{x^2}{\rho_1} \eta_3 a_{v7} = 0 \end{aligned} \quad (3.60)$$

$$\begin{aligned} & \frac{\beta}{\rho_2} \nu a_{v2} + \frac{\beta}{\rho_2} \nu a_{v3} - s_2 s_3 \frac{U_2^2}{W^2} \frac{\beta}{\rho_2} \nu a_{v4} - \sqrt{\frac{\mu_0}{\varepsilon_0}} k \frac{U_2^2}{\rho_2} \eta_4 a_{v6} - \sqrt{\frac{\mu_0}{\varepsilon_0}} k \frac{U_2^2}{\rho_2} \eta_5 a_{v7} \\ & + s_2 s_3 \sqrt{\frac{\mu_0}{\varepsilon_0}} k \frac{U_2^2}{\rho_2} \eta_6 a_{v8} = 0 \end{aligned} \quad (3.61)$$

$$\begin{aligned} & \sqrt{\frac{\varepsilon_0}{\mu_0}} k n_1^2 \frac{x}{\rho_1} \eta_1 a_{v1} - s_1 s_2 \sqrt{\frac{\varepsilon_0}{\mu_0}} k n_2^2 \frac{x^2}{\rho_1} a_{v2} \eta_2 - s_1 s_2 \sqrt{\frac{\varepsilon_0}{\mu_0}} k n_2^2 \frac{x^2}{\rho_1} a_{v3} \eta_3 \\ & - \nu \frac{\beta}{\rho_1} a_{v5} + s_1 s_2 \frac{x^2}{U_1^2} \frac{\beta}{\rho_1} \nu a_{v6} + s_1 s_2 \frac{x^2}{U_1^2} \frac{\beta}{\rho_1} \nu a_{v7} = 0 \end{aligned} \quad (3.62)$$

$$\begin{aligned} & \sqrt{\frac{\varepsilon_0}{\mu_0}} k n_2^2 \frac{U_2^2}{\rho_2} \eta_4 a_{v2} + \sqrt{\frac{\varepsilon_0}{\mu_0}} k n_2^2 \frac{U_2^2}{\rho_2} \eta_5 a_{v3} - s_2 s_3 \sqrt{\frac{\varepsilon_0}{\mu_0}} k n_3^2 \frac{U_2^2}{\rho_2} \eta_6 a_{v4} - \frac{\beta}{\rho_2} \nu a_{v6} \\ & - \frac{\beta}{\rho_2} \nu a_{v7} + s_2 s_3 \frac{U_2^2}{W^2} \nu \frac{\beta}{\rho_2} a_{v8} = 0 \end{aligned} \quad (3.63)$$

If we regard the eight coefficients $a_1, a_2, a_3, a_4, a_5, a_6, a_7, a_8$ as eight elements of column matrix \vec{I} , then the above eight linear equations could be expressed by the following form of matrix:

$$\vec{A}\vec{I} = \vec{O} \quad (3.64)$$

$$\begin{bmatrix}
1 & -1 & -1 & 0 & 0 & 0 & 0 & 0 & 0 \\
0 & 1 & 1 & -1 & 0 & 0 & 0 & 0 & 0 \\
0 & 0 & 0 & 0 & 1 & -1 & -1 & 0 & 0 \\
0 & 0 & 0 & 0 & 0 & 0 & 1 & -1 & -1 \\
\frac{v\beta}{\rho_1} & -\lambda_1 \lambda_2 \frac{U_1^2 v\beta}{U_2^2 \rho_1} & -\lambda_1 \lambda_2 \frac{U_1^2 v\beta}{U_2^2 \rho_1} & -\lambda_1 \lambda_2 \frac{U_1^2 v\beta}{U_2^2 \rho_1} & -\frac{\sqrt{\mu_0 k U_1^2}}{\sqrt{\varepsilon_0} \rho_1} \eta_1 & \lambda_1 \lambda_2 \sqrt{\frac{\mu_0 k U_1^2}{\varepsilon_0} \rho_1} \eta_2 & \lambda_1 \lambda_2 \sqrt{\frac{\mu_0 k U_1^2}{\varepsilon_0} \rho_1} \eta_3 & 0 & 0 \\
0 & \frac{v\beta}{\rho_2} & \frac{v\beta}{\rho_2} & \frac{v\beta}{\rho_2} & 0 & -\lambda_2 \lambda_3 \frac{U_3^2 v\beta}{W^2 \rho_2} & -\frac{\sqrt{\mu_0 k U_3^2}}{\sqrt{\varepsilon_0} \rho_2} \eta_4 & -\frac{\sqrt{\mu_0 k U_3^2}}{\sqrt{\varepsilon_0} \rho_2} \eta_5 & \lambda_2 \lambda_3 \sqrt{\frac{\mu_0 k U_3^2}{\varepsilon_0} \rho_2} \eta_6 \\
\frac{\sqrt{\varepsilon_0 k n_1^2} U_1}{\sqrt{\mu_0} \rho_1} \eta_1 & -\lambda_1 \lambda_2 \sqrt{\frac{\varepsilon_0 k n_2^2 U_1^2}{\mu_0} \rho_1} \eta_2 & -\lambda_1 \lambda_2 \sqrt{\frac{\varepsilon_0 k n_2^2 U_1^2}{\mu_0} \rho_1} \eta_3 & -\lambda_1 \lambda_2 \sqrt{\frac{\varepsilon_0 k n_2^2 U_1^2}{\mu_0} \rho_1} \eta_3 & \frac{v\beta}{\rho_1} & \lambda_1 \lambda_2 \frac{U_1^2 v\beta}{U_2^2 \rho_1} & \lambda_1 \lambda_2 \frac{U_1^2 v\beta}{U_2^2 \rho_1} & 0 & 0 \\
0 & \frac{\sqrt{\varepsilon_0 k n_2^2} U_3}{\sqrt{\mu_0} \rho_2} \eta_4 & \frac{\sqrt{\varepsilon_0 k n_2^2} U_3}{\sqrt{\mu_0} \rho_2} \eta_5 & -\lambda_2 \lambda_3 \sqrt{\frac{\varepsilon_0 k n_3^2 U_3^2}{\mu_0} \rho_2} \eta_6 & 0 & \frac{v\beta}{\rho_2} & \frac{v\beta}{\rho_2} & \lambda_2 \lambda_3 \frac{U_3^2 v\beta}{W^2 \rho_2} & \lambda_2 \lambda_3 \frac{U_3^2 v\beta}{W^2 \rho_2}
\end{bmatrix}
\begin{bmatrix}
a_{14} \\
a_{12} \\
a_{13} \\
a_{14} \\
a_{15} \\
a_{16} \\
a_{17} \\
a_{18}
\end{bmatrix}
= \begin{bmatrix} 0 \end{bmatrix}$$

(3.65)

\vec{O} is zero matrix.

The determinant of the matrix \vec{A} must vanish in order to have non-trivial solutions of the coefficients. A quadratic equation, i.e., the eigenvalue equation may be derived by an elimination process.^{8,9}

$$G_1\eta_1^2 + G_2\eta_1 + G_3 = 0 \quad (3.66)$$

where

$$\begin{aligned} G_1 &= ad - bc \\ G_2 &= (ad' - cb') + (da' - bc') \\ G_3 &= a'd' - b'c' \end{aligned} \quad (3.67)$$

with

$$a = \mu_2 \varepsilon_1 (\varepsilon_2 \Delta_2 - \varepsilon_3 \Delta_5) \quad (3.68)$$

$$a' = \varepsilon_2 AB (\xi - 1) - \mu_2 \varepsilon_2 (\varepsilon_2 \Delta_3 + \varepsilon_3 \Delta_1 \eta_6) \quad (3.69)$$

$$b = \mu_1 \varepsilon_2 (\xi - 1) B \quad (3.70)$$

$$b' = \mu_2 A (\varepsilon_2 \Delta_2 - \varepsilon_3 \Delta_5) + \mu_2 \varepsilon_2 \Delta_1 B \quad (3.71)$$

$$c = \mu_2 \varepsilon_1 (\xi - 1) B \quad (3.72)$$

$$c' = \varepsilon_2 A (\mu_2 \Delta_2 - \mu_3 \Delta_5) + \mu_2 \varepsilon_2 \Delta_1 B \quad (3.73)$$

$$d = \mu_1 \varepsilon_2 (\mu_2 \Delta_2 - \mu_3 \Delta_5) \quad (3.74)$$

$$d' = \mu_2 AB (\xi - 1) - \mu_2 \varepsilon_2 (\mu_2 \Delta_3 + \mu_3 \Delta_1 \eta_6) \quad (3.75)$$

and

$$\begin{aligned}
 \Delta_1 &= \eta_2 - \xi \eta_3 \\
 \Delta_2 &= \xi \eta_4 - \eta_3 \\
 \Delta_3 &= \xi \eta_3 \eta_4 - \eta_2 \eta_5 \\
 \Delta_4 &= \xi (\eta_2 - \eta_3) (\eta_4 - \eta_5) \\
 \Delta_5 &= (\xi - 1) \eta_6
 \end{aligned} \tag{3.76}$$

$$\begin{aligned}
 A &= \nu n_{eff} \left[\frac{s_1}{x^2} - \frac{s_2}{U_1^2} \right] \\
 B &= \nu n_{eff} \left[\frac{s_2}{U_2^2} - \frac{s_3}{W^2} \right]
 \end{aligned} \tag{3.77}$$

$$\xi = \frac{Z_{v,2}(U_2) Z_{v,3}(U_1)}{Z_{v,2}(U_1) Z_{v,3}(x)} \tag{3.78}$$

Solving this quadratic equation, two roots of η_i are obtained

$$\begin{aligned}
 \eta_i &= (1/2G_1) \left[-G_2 \pm (\delta)^{1/2} \right] \\
 \text{where } \delta &= G_2^2 - 4G_1G_3
 \end{aligned} \tag{3.79}$$

This is the eigenvalue equations of modes HE_{vm} and EH_{vm} .

In order to derive the cutoff and the far-from-cutoff conditions, the above equation is rewritten by redefining the $\eta_1, \eta_2, \eta_3, \eta_4, \eta_5, \eta_6$.

Through the following definitions of Bessel functions,

$$\begin{aligned}
 tB'_n(x) &= tB_{n-1}(x) - nB_n(x) \\
 tK'_n(x) &= -tK_{n-1}(x) - nK_n(x) \\
 B_n \text{ can be } &J_n(x), I_n(x), Y_n(x)
 \end{aligned} \tag{3.80}$$

Redefine:

$$\bar{\eta}_1 = \frac{s_1}{x} \frac{Z_{v-1,1}(x)}{Z_{v,1}(x)} \quad (3.81)$$

$$\bar{\eta}_2 = \frac{s_2}{U_1} \frac{Z_{v-1,2}(U_1)}{Z_{v,2}(U_1)} \quad (3.82)$$

$$\bar{\eta}_3 = \frac{1}{U_1} \frac{Z_{v-1,3}(U_1)}{Z_{v,3}(U_1)} \quad (3.83)$$

$$\bar{\eta}_4 = \frac{s_2}{U_2} \frac{Z_{v-1,2}(U_2)}{Z_{v,2}(U_2)} \quad (3.84)$$

$$\bar{\eta}_5 = \frac{1}{U_2} \frac{Z_{v-1,3}(U_2)}{Z_{v,3}(U_2)} \quad (3.85)$$

$$\bar{\eta}_6 = \frac{1}{W} \frac{K_{v-1}(W)}{K_v(W)} \quad (3.86)$$

and

$$\bar{\Delta}_1 = \bar{\eta}_2 - \xi \bar{\eta}_3 \quad (3.87)$$

$$\bar{\Delta}_2 = \xi \bar{\eta}_4 - \bar{\eta}_5 \quad (3.88)$$

$$\bar{\Delta}_3 = \xi \bar{\eta}_3 \bar{\eta}_4 - \bar{\eta}_2 \bar{\eta}_5 \quad (3.89)$$

$$\bar{\Delta}_4 = \xi (\bar{\eta}_2 - \bar{\eta}_3) (\bar{\eta}_4 - \bar{\eta}_5) \quad (3.90)$$

$$\bar{\Delta}_5 = (\xi - 1) \bar{\eta}_6 \quad (3.91)$$

where $\bar{x}^2 = s_1 x^2$, $\bar{U}_1^2 = s_2 U_1^2$, $\bar{U}_2^2 = s_2 U_2^2$, $\bar{W}^2 = s_3 W^2$

The eigenvalue equation is rewritten as:^{8 9}

$$\bar{\eta}_1 = \frac{\nu}{\bar{x}^2} + \left\{ -G_2 \pm \left[\left(G_2' \right)^2 + 4\varepsilon_1 (\varepsilon_2 T)^2 \right]^{1/2} \right\} / 2G_1 \quad (3.92)$$

where

$$\begin{aligned} G_1 &= \varepsilon_1 \varepsilon_2 H_1 \\ G_2 &= H_2 && \text{with the upper sign} \\ G_2' &= H_2 && \text{with the lower sign} \end{aligned} \quad (3.93)$$

$$T = \nu n_{eff} \left[\left(\frac{1}{\bar{x}^2} - \frac{1}{\bar{U}_1^2} \right) H_1 + \varepsilon_2 \left(\frac{1}{\bar{U}_2^2} - \frac{1}{\bar{W}^2} \right) \bar{\Delta}_4 \right] \quad (3.94)$$

$$\begin{aligned} H_1 &= (\varepsilon_2 \bar{\Delta}_2 - \varepsilon_3 \bar{\Delta}_5) (\bar{\Delta}_2 - \bar{\Delta}_5) \\ &- \nu (\xi - 1) \left\{ \frac{[2\varepsilon_2 \bar{\Delta}_2 - (\varepsilon_2 + \varepsilon_3) \bar{\Delta}_5]}{\bar{U}_2^2} - \frac{[(\varepsilon_2 + \varepsilon_3) \bar{\Delta}_2 - 2\varepsilon_3 \bar{\Delta}_5]}{\bar{W}^2} \right\} \end{aligned} \quad (3.95)$$

$$\begin{aligned} H_2 &= \varepsilon_2 \left\{ \nu (\varepsilon_1 \pm \varepsilon_2) \frac{H_1}{\bar{U}_1^2} - \nu \varepsilon_2 \bar{\Delta}_4 \left[\frac{(\varepsilon_1 \pm \varepsilon_2)}{\bar{U}_2^2} - \frac{(\varepsilon_1 \pm \varepsilon_3)}{\bar{W}^2} \right] \right. \\ &+ \nu (\varepsilon_1 \pm \varepsilon_2) (\xi - 1) \left[\bar{\Delta}_3 \left(\frac{2\varepsilon_2}{\bar{U}_2^2} - \frac{(\varepsilon_2 + \varepsilon_3)}{\bar{W}^2} \right) + \bar{\Delta}_1 \bar{\eta}_6 \left(\frac{(\varepsilon_2 + \varepsilon_3)}{\bar{U}_2^2} - \frac{2\varepsilon_3}{\bar{W}^2} \right) \right] \\ &\left. - \varepsilon_1 (\varepsilon_2 \bar{\Delta}_2 - \varepsilon_3 \bar{\Delta}_5) (\bar{\Delta}_3 + \bar{\Delta}_1 \bar{\eta}_6) \mp \varepsilon_2 (\bar{\Delta}_2 - \bar{\Delta}_5) (\varepsilon_2 \bar{\Delta}_3 + \varepsilon_3 \bar{\Delta}_1 \bar{\eta}_6) \right\} \end{aligned} \quad (3.96)$$

It has been shown⁹ that expression (3.92) is the eigenvalue equation for modes *EH* and *HE*, i.e. two groups of roots of the quadratic equation, “+” and “-” sign in the expressions make two groups of solutions represent two classes of hybrid modes, *EH* and *HE* modes respectively. The mode with zero cutoff frequency has been traditionally referred to as the *HE*₁₁ mode. Then the group of roots which might include zero cutoff frequency designates the mode *HE*.

3.2.6 Eigenvalue Equations of Modes *TE* and *TM*

As discussed in the two layer structures, transverse modes *TE* and *TM* are special situations of hybrid modes *HE* and *EH*. As $\nu = 0$, the eigenvalue equations of transverse modes *TE* and *TM* will be obtained from the eigenvalue equations of hybrid modes *HE* and *EH*.

The eigenvalue equation of modes *TE*

$$\bar{\eta}_1 (\bar{\Delta}_2 - \bar{\Delta}_5) - (\bar{\Delta}_3 + \bar{\Delta}_1 \bar{\eta}_6) = 0 \quad (3.97)$$

The eigenvalue equation of modes *TM*

$$\varepsilon_1 (\varepsilon_2 \bar{\Delta}_2 - \varepsilon_3 \bar{\Delta}_5) \bar{\eta}_1 - \varepsilon_2 (\varepsilon_2 \bar{\Delta}_3 + \varepsilon_3 \bar{\Delta}_1 \bar{\eta}_6) = 0 \quad (3.98)$$

3.3 Cutoff Conditions

We could derive the cutoff conditions of mode *TE* and *TM* from its eigenvalue equation in the limit of $W \rightarrow 0$, i.e. $n_{\text{eff}} \rightarrow n_3$. Under this condition, all the modes below the cutoff condition become radiation modes. n_3 is the refractive index of outer cladding of the fibre.

Letting $n_{\text{eff}} \rightarrow n_3$ i.e. $\alpha_3 \rightarrow 0$, the following small argument approximation in the

Table 4⁸ ⁹ will be used in the deduction related with the $\bar{\eta}_6 = K_{\nu-1}(W)/WK_{\nu}(W)$.

Table 4 The small argument approximation

ν	$\nu = 1$	$\nu \geq 2$	$\nu = 0$
$\frac{K_{\nu-1}(x)}{xK_{\nu}(x)}$	$\ln\left(\frac{2}{\gamma x}\right) \rightarrow \infty$	$\frac{1}{2(\nu-1)}$	$\frac{-1}{x^2 \ln\left(\frac{\gamma x}{2}\right)} \rightarrow \infty$

3.3.1 Cutoff Condition of Mode TE and TM

As $\nu = 0$, the modes, with one of whose longitudinal components equal to zero, are circularly symmetric modes and are called *TE* and *TM* modes.

As $W \rightarrow 0$, the $\bar{\eta}_6 \rightarrow \infty$ and $\bar{\Delta}_5 \rightarrow \infty$

For *TE* modes:

$$\bar{\eta}_1(\xi - 1) + \bar{\Delta}_1 = 0 \quad (3.99)$$

For *TM* modes:

$$\varepsilon_1 \bar{\eta}_1(\xi - 1) + \varepsilon_2 \bar{\Delta}_1 = 0 \quad (3.100)$$

3.3.2 Cutoff Condition of Mode HE and EH

As $\nu \geq 1$, we obtain^{8 9}:

$$\bar{\eta}_1 = \frac{\nu}{\bar{x}^2} + \left\{ E_2 \pm \sigma \left[(E_2')^2 + 4\varepsilon_1 \varepsilon_3 E_3^2 \right]^{1/2} \right\} / 2E_1 \quad (3.101)$$

where for $\nu > 1$

$$\begin{aligned}
E_1 &= -\varepsilon_1 C_1 \\
E_2 &= (\varepsilon_1 + \varepsilon_2) \left(\nu C_1 / \bar{U}_1^2 - C_2 \right) + \varepsilon_2 (\varepsilon_1 + \varepsilon_3) \bar{\Delta}_4 \\
E_2' &= (\varepsilon_1 - \varepsilon_2) \left(\nu C_1 / \bar{U}_1^2 - C_2 \right) + \varepsilon_2 (\varepsilon_1 - \varepsilon_3) \bar{\Delta}_4 \\
E_3 &= \nu C_1 \left(1/\bar{x}^2 - 1/\bar{U}_1^2 \right) - \varepsilon_2 \bar{\Delta}_4 \\
\sigma &= \text{sgn}(\xi - 1)
\end{aligned} \tag{3.102}$$

with

$$\begin{aligned}
C_1 &= (\xi - 1) \left[(\varepsilon_1 + \varepsilon_2) \bar{\Delta}_2 - \varepsilon_3 (\xi - 1) / (\nu - 1) \right] \\
C_2 &= (\xi - 1) \left[(\varepsilon_2 + \varepsilon_3) \bar{\Delta}_3 + \varepsilon_3 \bar{\Delta}_1 / (\nu - 1) \right]
\end{aligned} \tag{3.103}$$

And for $\nu = 1$

$$\begin{aligned}
E_1 &= \varepsilon_1 (\xi - 1) \\
E_2 &= -(\varepsilon_1 + \varepsilon_2) \left[\bar{\Delta}_1 + (\xi - 1) / \bar{U}_1^2 \right] \\
E_2' &= -(\varepsilon_1 - \varepsilon_2) \left[\bar{\Delta}_1 + (\xi - 1) / \bar{U}_1^2 \right] \\
E_3 &= (\xi - 1) \left(1/\bar{x}^2 - 1/\bar{U}_1^2 \right) \\
\sigma &= \text{sgn}(\xi - 1)
\end{aligned} \tag{3.104}$$

3.4 Far-from-cutoff Condition of Mode *HE* and *EH*

As modal parameter W tends to infinity, all the modal power is confined in the core. This is called the far-from-cutoff condition of mode in waveguides. No previous work on the derivation of the far-from-cutoff condition has been seen. This work aims at finding a proper limitation to

derive the far-from-cutoff condition from the eigenvalue equations of modes HE and EH . Satisfactory results have been obtained before in two layer structures at the limit of $W \rightarrow \infty$.

The defined modal parameters of dielectric waveguides (3.13) can be rewritten as:

$$\bar{x}^2 = (k\rho_1)^2 (n_1^2 - n_{eff}^2) \quad (3.105)$$

$$\bar{U}_1^2 = (k\rho_1)^2 (n_2^2 - n_{eff}^2) \quad (3.106)$$

$$\bar{U}_2^2 = (k\rho_2)^2 (n_2^2 - n_{eff}^2) \quad (3.107)$$

$$\bar{W}^2 = -(k\rho_2)^2 (n_{eff}^2 - n_3^2) \quad (3.108)$$

If $k\rho \rightarrow \infty$, W tends to infinity, i.e. the far-from-cutoff condition, but $\bar{x}, \bar{U}_1, \bar{U}_2$ remain finite, then the eigenvalue equation of three layer dielectric waveguides will develop into to the function of modal parameters $\bar{x}, \bar{U}_1, \bar{U}_2$

$$\lim_{\bar{W} \rightarrow \infty} f(\bar{x}, \bar{U}_1, \bar{U}_2) = 0 \quad (3.109)$$

With this limit $W \rightarrow \infty$, $\eta_6 \rightarrow 0$, we have $\Delta_s = (\xi - 1)$ and $\eta_6 \rightarrow 0$, the far-from-cutoff expression will be derived in next section.

3.4.1 Far-from-cutoff Condition of TE and TM mode

For TE modes:

$$\bar{\eta}_1 \bar{\Delta}_2 - \bar{\Delta}_3 = 0 \quad (3.110)$$

For TM modes:

$$\varepsilon_1 \bar{\eta}_1 \bar{\Delta}_2 - \varepsilon_2 \bar{\Delta}_3 = 0 \quad (3.111)$$

3.4.2 Far-from-cutoff Condition of HE and EH modes

To achieve the proposal of finding the other boundary to form a value range, this work deducts the far-from-cutoff condition of modes in three layer structures with the help of the eigenvalue equation given by *Safaai-Jazi and Yip's*.^{8 9}

For the hybrid modes, $\nu > 0$, the eigenvalue equations are rewritten as follow:

$$\bar{\eta}_1 = \frac{\nu}{\bar{x}^2} + \frac{-E_2 \pm \left[(E_2')^2 + 4\varepsilon_1 E_3^2 \right]^{1/2}}{E_1} \quad (3.112)$$

where

$$\begin{aligned} E_1 &= 2\varepsilon_1 D_1 \\ E_2 &= (\varepsilon_1 + \varepsilon_2) D_2 \\ E_2' &= (\varepsilon_1 - \varepsilon_2) D_2 \\ E_3 &= \nu n_{eff} \left[\left(\frac{1}{\bar{x}^2} - \frac{1}{\bar{U}_1^2} \right) D_1 + \frac{\varepsilon_2}{\bar{U}_2^2} \bar{\Delta}_4 \right] \end{aligned} \quad (3.113)$$

with

$$\begin{aligned}
 D_1 &= \varepsilon_2 \left(\bar{\Delta}_2 - \frac{2\nu(\xi-1)}{\bar{U}_2^2} \right) \bar{\Delta}_2 \\
 D_2 &= \frac{\nu}{\bar{U}_1^2} D_1 - \frac{\nu\varepsilon_2}{\bar{U}_2^2} [\bar{\Delta}_4 - 2(\xi-1)\bar{\Delta}_3] - \varepsilon_2 \bar{\Delta}_2 \bar{\Delta}_3
 \end{aligned} \tag{3.114}$$

The sign “+” represents the far-from-cutoff conditions of modes EH, and “−” represents the far-from-cutoff conditions of modes HE respectively.

Numerical calculations have been conducted to verify the validity of the above far-from-cutoff obtained from the limit of $W \rightarrow \infty$. The numerical calculation results show that the cutoff condition obtained at the limit of $W \rightarrow 0$ and the far-from-cutoff condition obtained at the limit of $W \rightarrow \infty$ can form a closed value range which includes the effective index of mode *HE* or *EH*.

CHAPTER 4

VERIFICATION, NUMERICAL CALCULATION

4.1 Transition from three layer to two layer

If we let $b \rightarrow a$, the three layer fibre structure will shrink to a typical two layer fibre structure. Comparing the reduced eigenvalue equation, the cutoff and the far-from-cutoff conditions with the results obtained in the Chapter 2, we can verify the validity of the results obtained in Chapter 3.

As $b \rightarrow a$, we will have

$$\begin{aligned}\bar{U}_2 &\rightarrow \bar{U}_1 \\ \bar{\eta}_4 &\rightarrow \bar{\eta}_2 \\ \bar{\eta}_5 &\rightarrow \bar{\eta}_3 \\ \xi &\rightarrow 1\end{aligned}\tag{4.1}$$

and

$$\begin{aligned}\bar{\Delta}_5 &\rightarrow 0 \\ \bar{\Delta}_3 &\rightarrow 0 \\ \bar{\Delta}_4 &\rightarrow (\bar{\eta}_2 - \bar{\eta}_3) \\ \bar{\Delta}_2 &\rightarrow \bar{\Delta}_1\end{aligned}\tag{4.2}$$

4.1.1 Eigenvalue Equation

Substituting equation (4.1) and (4.2) into the eigenvalue equation (3.92), the eigenvalue equation of three layer cladded fibre will reduce to

$$(\mu_1 \bar{\eta}_1 - \mu_3 \bar{\eta}_6)(\varepsilon_1 \bar{\eta}_1 - \varepsilon_3 \bar{\eta}_6) = \left[\nu n_{eff} \left(\frac{1}{\bar{U}_1^2} + \frac{1}{\bar{W}^2} \right) \right]^2 \quad (4.3)$$

It is the same with eigenvalue equation (2.28) obtained in the two layer structures of Chapter 2.

4.1.2 Cutoff Condition

For $\nu = 0$, the cutoff condition of modes *HE* and *EH* in three layer fibre can be rewritten as follows:

$$\begin{cases} 0 \cdot \bar{\eta}_1 + \bar{\Delta}_1 = 0 & TE \\ \varepsilon_1 \cdot 0 \cdot \bar{\eta}_1 + \varepsilon_2 \bar{\Delta}_1 = 0 & TM \end{cases} \quad (4.4)$$

But, due to

$$\bar{\Delta}_1 = \bar{\eta}_2 - \xi \bar{\eta}_3 = \bar{\eta}_2 - \bar{\eta}_3 = \frac{1}{\alpha_2 a} \frac{I_{\nu-1}(\alpha_2 a)}{I_\nu(\alpha_2 a)} - \frac{1}{\alpha_2 a} \frac{K_{\nu-1}(\alpha_2 a)}{K_\nu(\alpha_2 a)} \neq 0$$

So, we must have $\bar{\eta}_1 \rightarrow \infty$ to keep equation(4.4) true, then

$$\begin{aligned} \bar{\eta}_1 &\rightarrow \infty \\ \frac{1}{\alpha_1 a} \frac{J_{\nu-1}(\alpha_1 a)}{J_\nu(\alpha_1 a)} &= \frac{1}{\alpha_1 a} \frac{J_{-1}(\alpha_1 a)}{J_0(\alpha_1 a)} \rightarrow \infty \\ J_0(\alpha_1 a) &= 0 \quad \text{for } TE \text{ or } TM \end{aligned} \quad (4.5)$$

For $\nu > 0$, the cutoff condition for three layer structures, applying

the same assumption as previously discussed for modes TE and TM in two layer structures, the cutoff condition (3.101) is rewritten as:

$$2E_1\eta_1 = \varepsilon_2(\varepsilon_1 + \varepsilon_3)\bar{\Delta}_4 \pm \sigma\varepsilon_2\bar{\Delta}_4(\varepsilon_1 + \varepsilon_3) \quad (4.6)$$

For EH modes,

$$2E_1\eta_1 = \varepsilon_2(\varepsilon_1 + \varepsilon_3)\bar{\Delta}_4 + \sigma\varepsilon_2\bar{\Delta}_4(\varepsilon_1 + \varepsilon_3) \rightarrow 0$$

$$\eta_1 \rightarrow 0$$

$$J_\nu(\alpha_1 a) = 0 \quad (4.7)$$

For HE modes,

$$2E_1\eta_1 = \varepsilon_2(\varepsilon_1 + \varepsilon_3)\bar{\Delta}_4 - \sigma\varepsilon_2\bar{\Delta}_4(\varepsilon_1 + \varepsilon_3) \rightarrow 0$$

$$\eta_1 \rightarrow \text{finite value} \quad (4.8)$$

Because $\xi \rightarrow 1$, we have $C_1, C_2 \rightarrow 0$, then $E_1 \rightarrow 0$. It will prove very simply and directly that the reduced cutoff conditions of modes HE and EH , including the transverse modes TE and TM , coincide exactly with the cutoff conditions we obtained in two layer structure fibre.

4.1.3 Far-from-cutoff Condition

With conditions (4.1) and (4.2),

$$\begin{aligned}
D_1 &= \varepsilon_2 \left(\bar{\Delta}_2 - \frac{2\nu(\xi-1)}{\bar{U}_2^2} \right) \bar{\Delta}_2 \rightarrow \varepsilon_2 \bar{\Delta}_2 \bar{\Delta}_2 \\
&\rightarrow \varepsilon_2 \bar{\Delta}_1^2
\end{aligned} \tag{4.9}$$

And

$$\begin{aligned}
D_2 &= \frac{\nu}{\bar{U}_1^2} D_1 - \frac{\nu \varepsilon_2}{\bar{U}_2^2} [\bar{\Delta}_4 - 2(\xi-1)\bar{\Delta}_3] - \varepsilon_2 \bar{\Delta}_2 \bar{\Delta}_3 \\
&\rightarrow \frac{\nu}{\bar{U}_1^2} D_1 - \frac{\nu \varepsilon_2}{\bar{U}_2^2} \bar{\Delta}_4 \\
&\rightarrow \frac{\nu}{\bar{U}_1^2} D_1 - \frac{\nu \varepsilon_2}{\bar{U}_2^2} \bar{\Delta}_1^2 \rightarrow 0
\end{aligned} \tag{4.10}$$

$$E_1 = 2\varepsilon_1 D_1 \rightarrow 2\varepsilon_1 \varepsilon_2 \bar{\Delta}_1^2 \tag{4.11}$$

$$E_2 = (\varepsilon_1 + \varepsilon_2) D_2 \rightarrow 0 \tag{4.12}$$

$$E_2' = (\varepsilon_1 - \varepsilon_2) D_2 \rightarrow 0 \tag{4.13}$$

$$\begin{aligned}
E_3 &= \nu n_{eff} \left[\left(\frac{1}{\bar{x}^2} - \frac{1}{\bar{U}_1^2} \right) \varepsilon_2 \bar{\Delta}_1^2 + \frac{\varepsilon_2}{\bar{U}_1^2} \bar{\Delta}_1^2 \right] \\
&\rightarrow \frac{\varepsilon_2 \nu n_{eff}}{\bar{x}^2} \bar{\Delta}_1^2
\end{aligned} \tag{4.14}$$

We will have:

$$\begin{aligned}
\bar{\eta}_1 &= \frac{\nu}{\bar{x}^2} + \frac{\pm \left[4\varepsilon_1 \left(\frac{\varepsilon_2 \nu n_{eff}}{\bar{x}^2} \bar{\Delta}_1^2 \right)^2 \right]^{1/2}}{2\varepsilon_1 \varepsilon_2 \bar{\Delta}_1^2} \\
&= \frac{\nu}{\bar{x}^2} + \frac{\pm \left[\left(\frac{2\varepsilon_1 \varepsilon_2 \nu}{\bar{x}^2} \bar{\Delta}_1^2 \right)^2 \right]^{1/2}}{2\varepsilon_1 \varepsilon_2 \bar{\Delta}_1^2} = \frac{\nu}{\bar{x}^2} \pm \frac{\frac{2\varepsilon_1 \varepsilon_2 \nu}{\bar{x}^2} \bar{\Delta}_1^2}{2\varepsilon_1 \varepsilon_2 \bar{\Delta}_1^2} \\
&= \frac{\nu}{\bar{x}^2} \pm \frac{\nu}{\bar{x}^2}
\end{aligned} \tag{4.15}$$

where

$$\bar{\eta}_1 = \frac{1}{\bar{x}} \frac{J_{\nu-1}(x)}{J_{\nu}(x)} \quad (4.16)$$

We rewrite the equation(4.15) as follow:

$$\begin{aligned} \bar{\eta}_1 - \frac{\nu}{(\alpha_1 a)^2} &= \pm \frac{\nu}{(\alpha_1 a)^2} \\ \eta_1 &= \pm \frac{\nu}{(\alpha_1 a)^2} \end{aligned} \quad (4.17)$$

$$\frac{J'_{\nu}(\alpha_1 a)}{U J_{\nu}(\alpha_1 a)} = \pm \frac{\nu}{(\alpha_1 a)^2} \quad (4.18)$$

Substituting the definition of Bessel function into the equation(4.18), we have:

$$\frac{J'_{\nu}(U)}{U J_{\nu}(U)} = \begin{cases} \frac{\nu}{U^2} - \frac{J_{\nu+1}(U)}{U J_{\nu}(U)} \\ \frac{J_{\nu-1}(U)}{U J_{\nu}(U)} - \frac{\nu}{U^2} \end{cases} \quad (4.19)$$

We will obtain the far-from-cutoff conditions as follow:

$$\begin{aligned} \frac{J_{\nu+1}(\alpha_1 a)}{U J_{\nu}(\alpha_1 a)} &\rightarrow 0 \\ \text{or} & \\ \frac{J_{\nu-1}(\alpha_1 a)}{U J_{\nu}(\alpha_1 a)} &\rightarrow 0 \end{aligned} \quad (4.20)$$

Furthermore, we could transform the far-from-cutoff condition as follow:

$$J_1(\alpha_1 a) = 0 \quad (\alpha_1 a \neq 0) \quad \text{Mode } TE_{0m} TM_{0m} \quad (4.21)$$

and

$$\begin{cases} J_{\nu-1}(\alpha_1 a) = 0 & (\alpha_1 a \neq 0) & \text{Mode } HE_{\nu m} \\ J_{\nu+1}(\alpha_1 a) = 0 & (\alpha_1 a \neq 0) & \text{Mode } EH_{\nu m} \end{cases} \quad (4.22)$$

It is identical to the far-from-cutoff condition of a two layer structure in Table 2 obtained in Chapter 2. It is proved that the two layer dielectric structure is a special case of a three layer structure. It proves to some extent that the obtained far-from-cutoff condition of three layer structures is true.

4.2 Numerical Calculation of the value range

4.2.1 Introduction

As in the eigenvalue equation, the cutoff and the far-from-cutoff equations obtained in three layer structure are all functions of modal parameters $\bar{x}, \bar{U}_1, \bar{U}_2$.

The cutoff equation:

$$\lim_{x \rightarrow \infty} f(\bar{x}, \bar{U}_1, \bar{U}_2) = 0 \quad (4.23)$$

The far-from-cutoff equation:

$$\lim_{x \rightarrow 0} f(\bar{x}, \bar{U}_1, \bar{U}_2) = 0 \quad (4.24)$$

The discrete solutions to the above equations are the cutoff and the far-from-cutoff conditions, which are all functions of effective index.

Like the n_{eff} (cutoff) and n_{eff} (far-from-cutoff) in two layer structures discussed before, the cutoff and far-from-cutoff conditions obtained in three layer structures have the corresponding effective indices, n_{eff} (cutoff) and n_{eff} (far-from-cutoff).

To find the roots of the eigenvalue, the cutoff and the far-from-cutoff equations, we use the *Brent* root finding method to find the effective index or the corresponding effective indices between the n_{max} and n_{min} . The n_{max} and n_{min} we use in the calculation are the indices of the core and the second cladding of the fibre. The first found root of the eigenvalue equation is the effective index of the eigenvalue equation, whereas the first found roots of the cutoff and the far-from-cutoff equations are the corresponding effective indices of the cutoff and the far-from-cutoff conditions.

We plot the corresponding effective indices of the cutoff and the far-from-cutoff conditions, n_{eff} (cutoff) and n_{eff} (far-from-cutoff) with the effective index of modes together to show that the effective index varies in the range formed by the n_{eff} (cutoff) and n_{eff} (far-from-cutoff).

Through the numerical calculation of the eigenvalue, the cutoff

and the far-from-cutoff equation, we proved that the obtained cutoff condition could be regarded as a boundary of the range which includes the effective index.

All calculations are based on the fibre *SMF-28*TM at the wavelength $\lambda=1.55\mu\text{m}$.

We plot the effective index, the corresponding effective indices of the cutoff and the far-from-cutoff conditions vs. the reduction factor *R*. The reduction factor *R* is a homothetic reduction factor of the transversal dimensions of the fibre.

Table 5 The definition of fibre *SMF-28*TM

Layer	Refractive index of layer	Radius
1	$SiO_2+0.0045 = 1.448918$	$4.5\mu\text{m}$
2	$SiO_2 = 1.444418$	$62.5\mu\text{m}$
3	$Air = 1.000273$	∞

4.2.2 Plot of Modes *TE* and *TM*

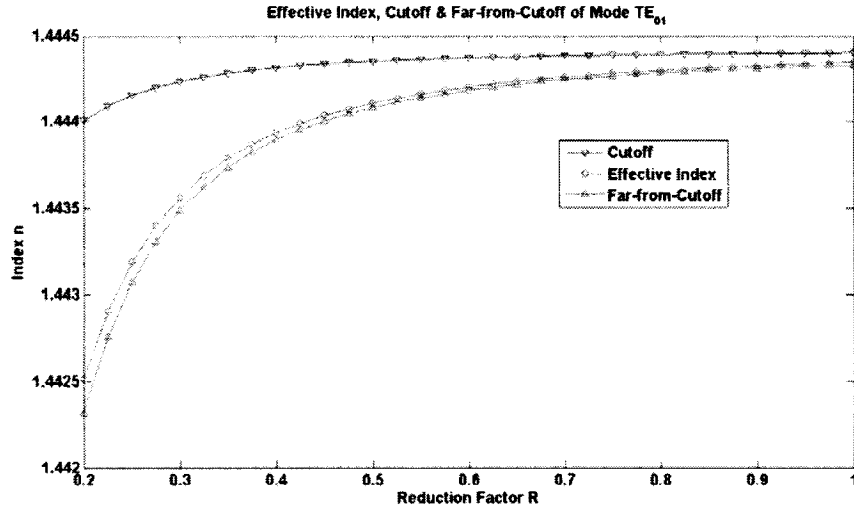


Fig. 8 Plot of effective index, far-from-cutoff condition of mode TE_{01} .

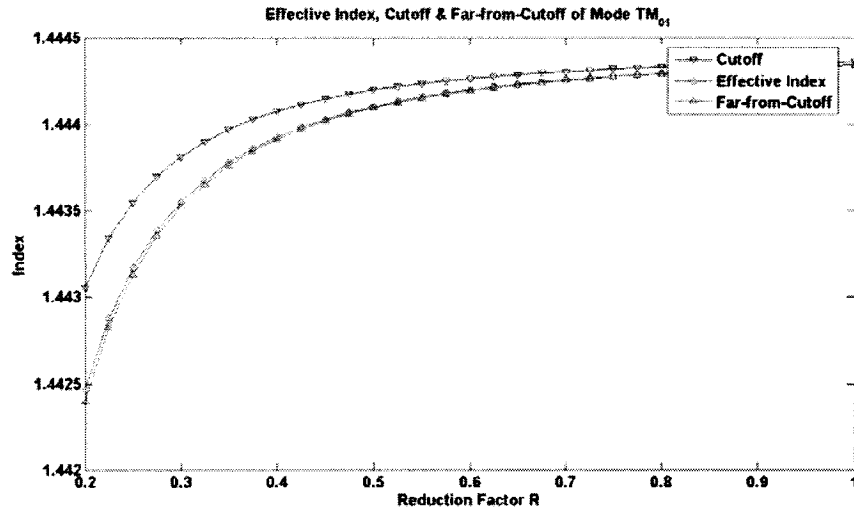


Fig. 9 Plot of effective index, far-from-cutoff condition of mode TM_{01} .

Fig. 8 Plot of effective index, far-from-cutoff condition of mode TE_{01} is the plot of effective index, cutoff and far-from-cutoff conditions of mode TE_{01} corresponding to the equation (3.97), (3.99) and (3.110) respectively.

Fig. 9 is the plot of effective index, cutoff and far-from-cutoff conditions of mode TM_{01} corresponding to the equation (3.98), (3.100) and (3.111) respectively.

4.2.3 Plot of Modes HE

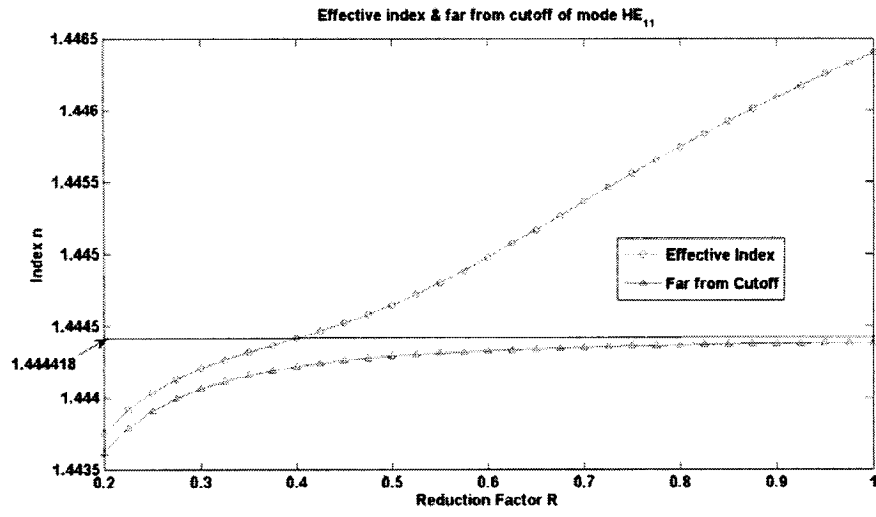


Fig. 10 Plot of effective index, far-from-cutoff condition of mode HE_{11} .

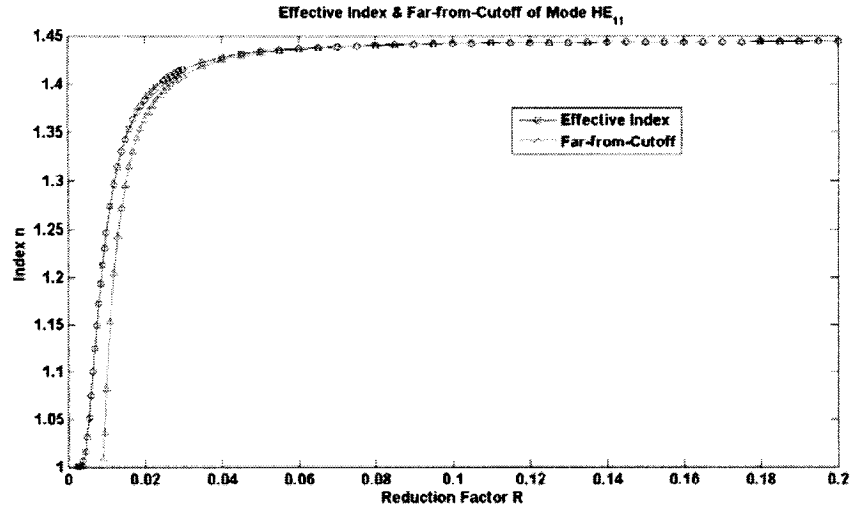


Fig. 11 Extended plot of mode HE_{11} .

Fig. 10 is the plot of the numerical results of equation (3.92), (3.101) and (3.112) vs. the reduction factor “ R ”. From the figure, we find that there is no cutoff for the mode HE_{11} . The effective index tends to the refractive index of the core. The mode HE_{11} always exists in the dielectric waveguide.

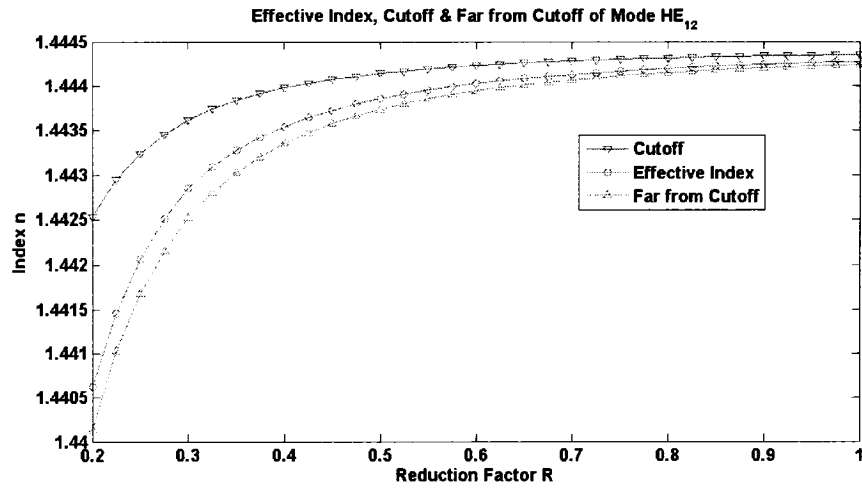


Fig. 12 Plot of effective index, cutoff and far from cutoff conditions of mode HE_{12} .

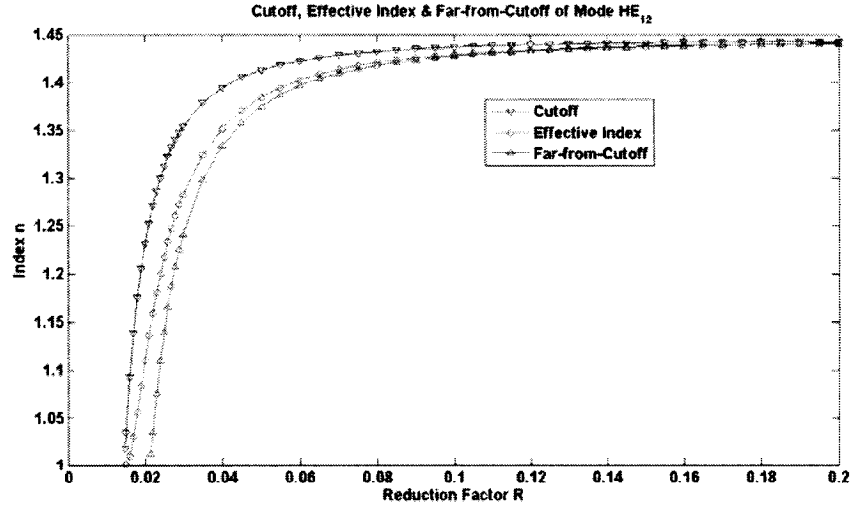


Fig. 13 Extended plot of mode HE_{12} .

Fig. 12 is the plot of effective index, cutoff and far-from-cutoff condition of mode HE_{12} vs. reduction factor, based on the same equation than the Fig. 10. From Fig. 14, we see that the effective index is bound in a value range formed by the cutoff and the far-from-cutoff conditions. From Fig. 11 and Fig. 13, we find that there is no cutoff for the mode HE_{11} , but mode HE_{12} will be cutoff as R approaches 0.01. For a given v , the mode, the cutoff and the far-from-cutoff values of the higher order of mode “ m ” will be cutoff earlier than the lower order of mode “ m ” as the R tends to zero. And the effective index is still bound in a value range formed by the cutoff and the far-from-cutoff conditions.

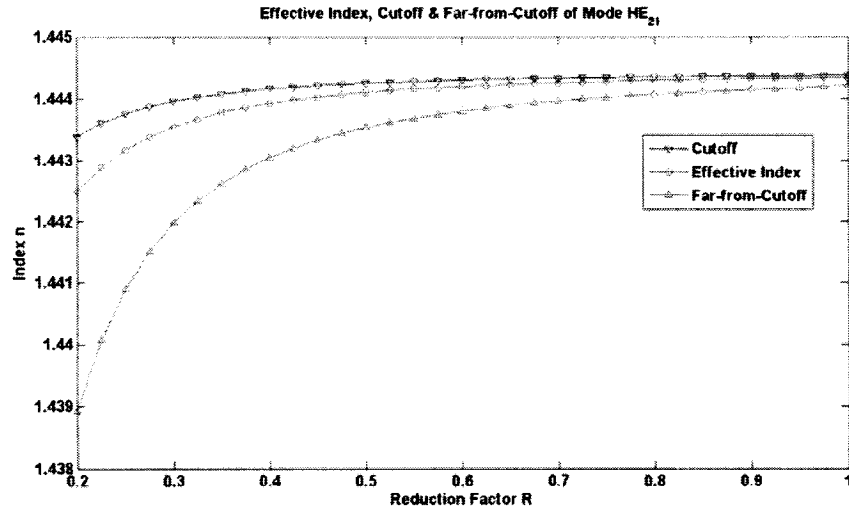


Fig. 14 Plot of effective index, cutoff and far-from-cutoff conditions of mode HE_{21} .

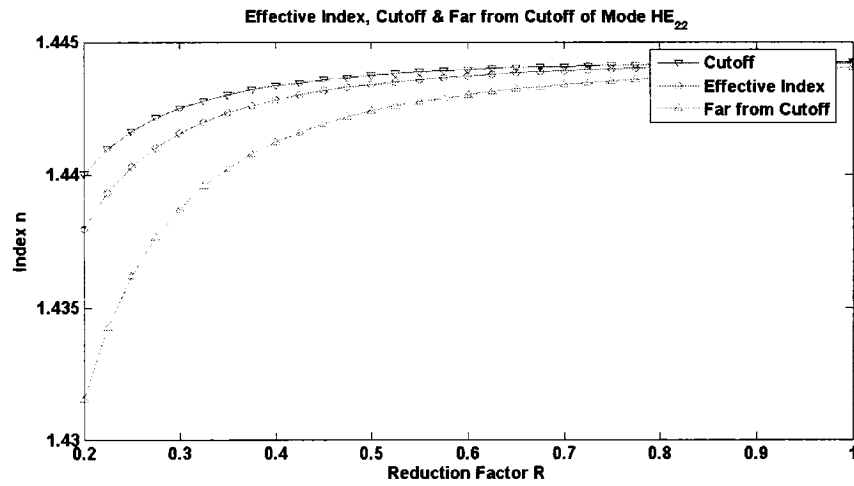


Fig. 15 Plot of effective index, cutoff and far-from-cutoff conditions of mode HE_{22} .

Fig. 14 and Fig. 15 show the effective index, cutoff and far-from-cutoff conditions of mode HE_{21} and HE_{22} . It is observed that the effective index varies in the region formed by the cutoff and the far-from-cutoff conditions.

4.2.4 Plot of Modes EH

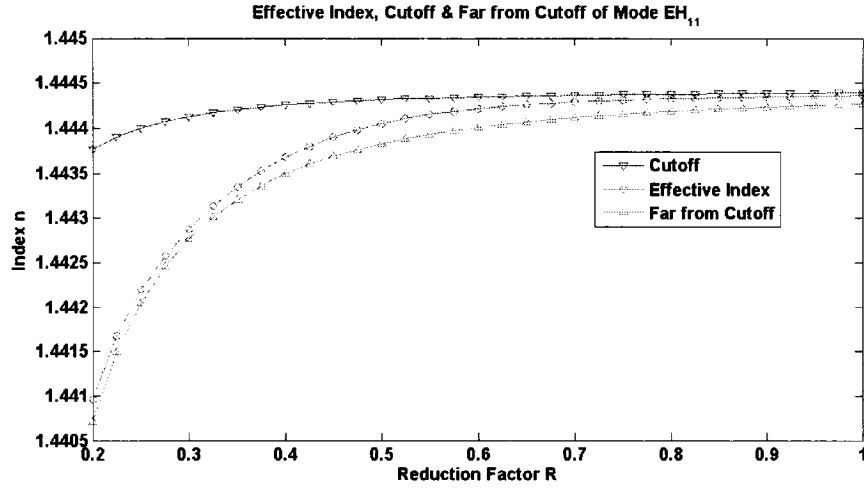


Fig. 16 Plot of effective index, cutoff and far-from-cutoff condition of mode EH_{11} .

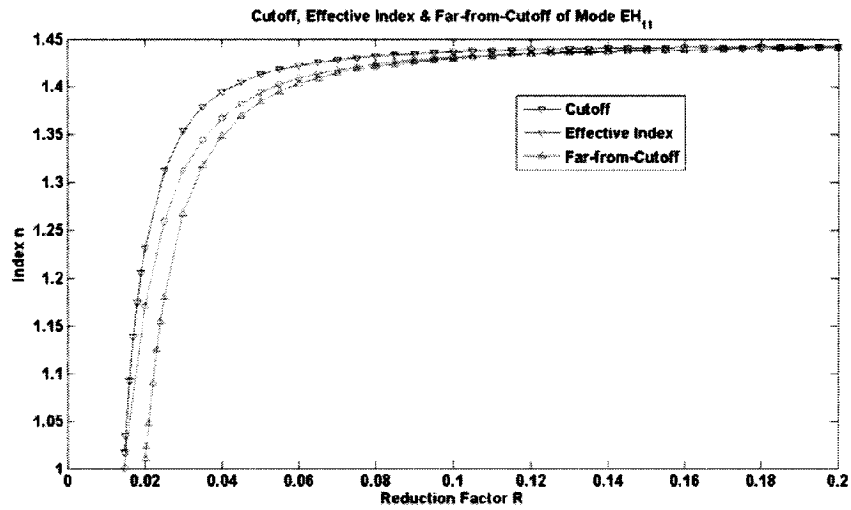


Fig. 17 Extended plot of mode EH_{11} .

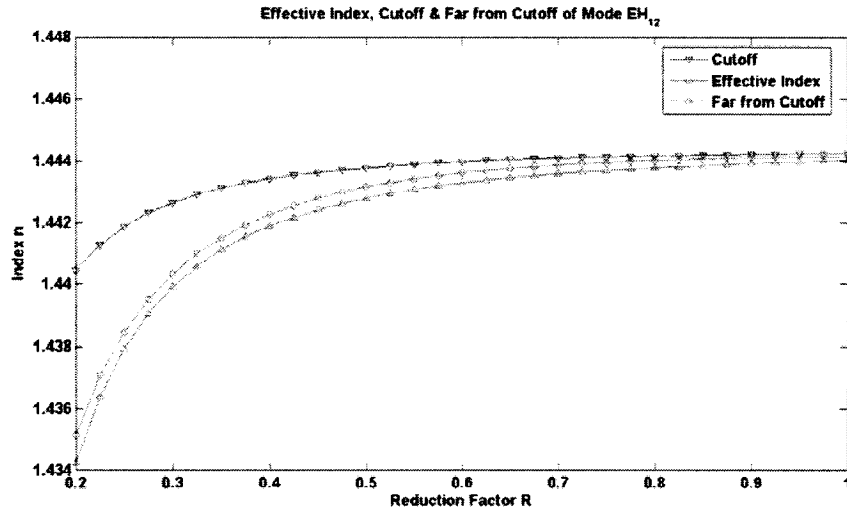


Fig. 18 Plot of effective index, cutoff and far-from cutoff conditions of mode EH_{12} .

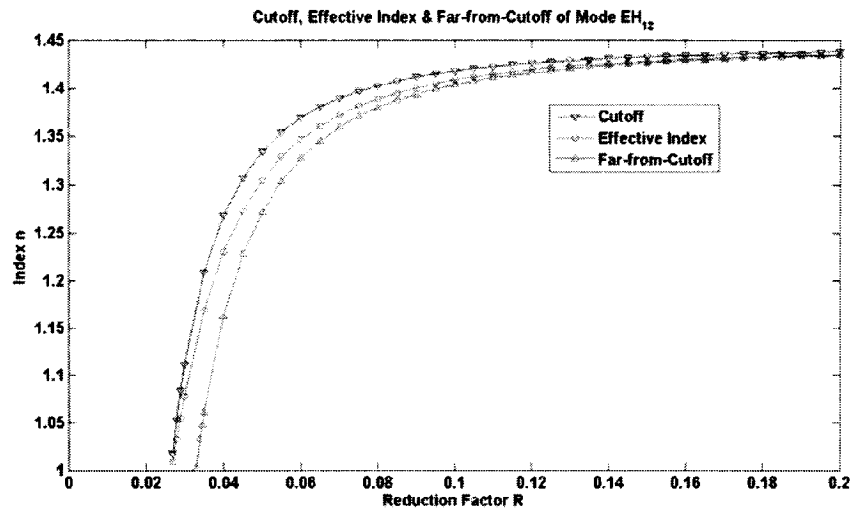


Fig. 19 Extended plot of mode EH_{12} .

Fig. 16 and Fig. 18 are plots of effective index, cutoff and far-from-cutoff conditions of mode EH_{11} and EH_{12} corresponding to the equation (3.92), (3.101) and (3.112). We see that the effective index is surrounded by the cutoff and the far-from-cutoff conditions.

4.2.5 Plot of value ranges of modes

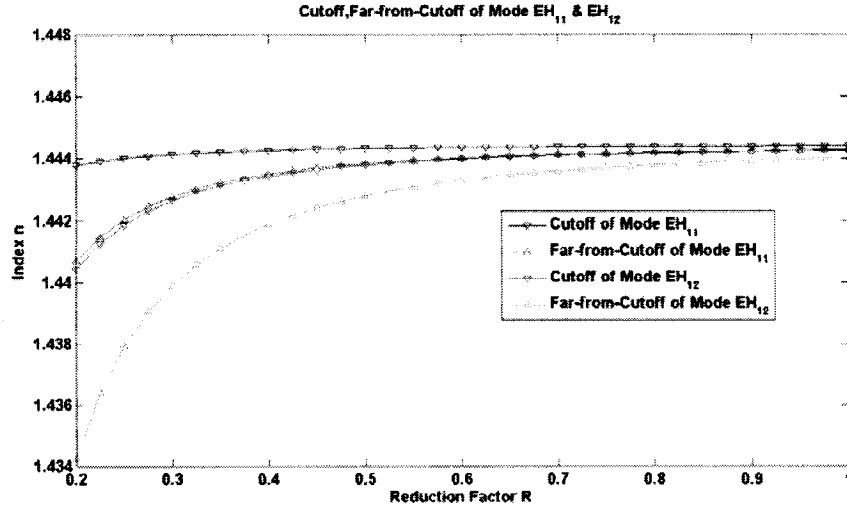


Fig. 20 Plot of value ranges of modes EH_{11} and EH_{12} .

Fig. 20 is the plot of the cutoff and the far-from-cutoff conditions of modes EH_{11} and EH_{12} . We plot the value range bounded by the cutoff and the far-from-cutoff conditions of two modes for a given $\nu=1$ to prove that two value ranges don't overlap.

4.3 Discussion

Like the situation in the two layer structure fibre, the effective index of modes is within the value range formed by the cutoff and the far-from-cutoff conditions. The eigenvalue, the cutoff and the far-from-cutoff equations include many terms of the complicated Bessel

function. The Bessel function, especially the higher order Bessel function makes the terms of the equation vary dramatically. It makes the function change sign many times in the tiny section of *Brent's* method or Bisection method. *Brent's* or Bisection method is a root-finding method. If the curves of the function changes too considerably, it is very hard to find a section which permits the function to change sign only one time in the tolerance of computer. The accuracy of used *Brent's* or Bisection method is set around the order of $10^{-17\sim-18}$. The numerical computation in this order of accuracy will take a very long time, but it still makes some errors, like missing some roots.

CHAPTER 5

CONCLUSION

From the deduction of Chapter 3, the eigenvalue, the cutoff and the far-from-cutoff equations of a guided mode in the three layer dielectric waveguides is obtained. The far-from-cutoff equations of modes (3.110), (3.111), (3.112) have never been obtained in previous papers. The obtained far-from-cutoff makes it possible to form a value range with the obtained cutoff obtained in the article.^{8 9} The eigenvalue of mode is between this value range. In other words, the eigenvalue or effective index is confined in the range formed by the cutoff and the far-from-cutoff conditions.

To prove the justness of the obtained cutoff and far-from-cutoff conditions of modes in three layer structures, we reduce the three layer to two layer by letting $b \rightarrow a$. The reduced cutoff and far-from-cutoff expressions are identical to the cutoff and far-from-cutoff expressions.

Chapter 4 gives some plots of effective index, cutoff and far-from-cutoff conditions of mode $HE_{\nu m}$ and $EH_{\nu m}$ ($\nu = 1, 2$, $m = 1, 2$) vs. reduction factor R . The plots show us that the effective index of mode

varies between the cutoff and the far-from-cutoff conditions. And we can observe from the extended plots that it is still true as R tends to zero.

The value range which includes effective makes it more convenient to investigate the effective index of mode analytically and numerically.

It is found from Fig. 20, the plot of the cutoff and far-from-cutoff conditions of modes EH_{11} and EH_{12} , that there is no overlapping of the value ranges of both modes of the same order.

It is proved numerically that the value ranges of each mode of the same order don't overlap; furthermore, the modes of the same order don't cross.

It is still very difficult to solve the eigenvalue, the cutoff and the far-from-cutoff equations. We think that it may be possible to find a value range which could include the cutoff or the far-from-cutoff values, which are the boundaries of value range including the effective index.

Until now, we have discussed the classification of modes in two and three layer structures. The four components of field in the four layer fibre, one core with three claddings, have to be continuous in three interfaces. Applying the same method used in two and three layer structures, we will obtain a 12×12 matrix. To set the determinant of this

matrix to be zero, we will get a quadratic equation too¹⁶. Solving this quadratic equation will lead to two group of roots, which present the modes EH and HE in four layer structures respectively. Choosing proper modal parameters, the quadratic equation can be transformed to the eigenvalue equation of modes in four layer structures, then the cutoff and the far-from-cutoff conditions consequently.

Reference

- ¹ S. E. Miller (1969), "Integrated optics: An Introduction," *Bell Syst. Tech. J.*, Vol. 48, p. 2059-2069, Sept.
- ² D. Marcuse (1972), "*Light Transmission Optics*". New York: Van Nostrand Reinhold.
- ³ P. K. Tien (1971), "Light waves in thin films and integrated optics," *Appl. Opt.*, vol. 10, p. 2395.
- ⁴ N. S. Kapany (1967), "*Fibre Optics*". New York: Academic.
- ⁵ E. Snitzer (1961), "Cylindrical dielectric waveguide modes," *J. Opt. Soc. Amer. Vol. 51*, pp. 491-498.
- ⁶ N.S. Kapany & J.J. Burke (1972), "Optical Waveguides". New York: Academic.
- ⁷ A.W. Snyder & J. D. Love (1993), "*Optical Waveguide Theory*," London, Chapman and Hall.
- ⁸ A. Safaai-Jazi & G .L .Yip (1977), "Classification of hybrid modes in cylindrical dielectric optical waveguides", *Radio Science, Vol. 12, No. 4*, pp. 603-609.
- ⁹ A. Safaai-Jazi & G .L .Yip (1978), "Cutoff Conditions in three-layer cylindrical dielectric optical waveguides", *IEEE Transaction on Microwave and Electronics,, Vol. MTT-26, No. 11*, pp. 898-903.
- ¹⁰ R.E. Beam, H.M. Asratom. W.C. Jakes, H.M. Wachowski, and W.L. Firestone (1949), "*Dielectric tube waveguides*," Northwestern Univ., Evanston, IL, Rep. ATT 94929,
- ¹¹ P. J. B. Clarricoats (1961), "Propagation along unbounded and bounded dielectric rods," *Proc. Inst. Elec. Eng. Vol. 108*, pp. 170-176.

-
- ¹² P. J. B. Clarricoats and K. B. Chan (1973), "Propagation behavior of cylindrical dielectric-rod waveguides," *Proc. Inst. Elec. Eng.*, vol. 120, no. 11, pp. 1371-1378.
- ¹³ M.M.Z. Kharadly and J.E. Lewis (1969), "Properties of dielectric tube waveguides," *Proc. Inst. Elec. Eng.*, vol. 116, pp. 214-224.
- ¹⁴ Achint Kapoor and G.S. Singh (2000), "Mode Classification in Cylindrical Dielectric Waveguide", *J. Lightwave Technology*, Vol. 18, No. 5, pp. 849-852.
- ¹⁵ M. Abramowitz and I. A. Stegun (1970), "*Handbook of Mathematical Functions, with formulas, graphs, and mathematical tables*": Dover Publications, INC., New York
- ¹⁶ A. Safaai-Jazi, R.O. Claus, and L. J. Lu (1989), "New designs for dispersion-shifted and dispersion-flattened fibres," *SPIE*, vol. 1176, pp. 196-201.
- ¹⁷ J. Bures, "*Technologie de l'optique guidée*," notes de cours, Département de génie physique, Presses internationales Polytechnique, Janvier 2006.